BAYESWAVE ANALYSIS STUDY ON RECOVERING WAVEFORM COMPLEXITY THROUGH RECONSTRUCTIONS

A Thesis
Presented to
The Academic Faculty

by

Brian Day

In Partial Fulfillment
of the Requirements for the Degree
Bachelors' of Science in Physics with the Research Option in the
College of Sciences, School of Physics

Georgia Institute of Technology
May 2017

BAYESWAVE ANALYSIS STUDY ON RECOVERING WAVEFORM COMPLEXITY THROUGH RECONSTRUCTIONS

Approved by:

Dr. Deirdre Shoemaker, Advisor
School of Physics
Georgia Institute of Technology

Dr. Pablo Laguna
School of Physics
Georgia Institute of Technology

Date Approved: April 26, 2017

ACKNOWLEDGEMENTS

I would like to thank Dr. Deirdre Shoemaker for assisting me with my research and for giving me the opportunity to be a part of undergraduate research while at the Georgia Institute of Technology. I would also like to thank Dr. James Clark for his assistance and guidance whenever I had an issue with my programs.

TABLE OF CONTENTS

LIST OF FIGURES

LIST OF SYMBOLS AND ABBREVIATIONS

LIGO	Laser Interferometer Gravitational-Wave Observatory
EOBNR	Equivalent-one-body model tuned to numerical relativity
cWB	Coherent Wave Burst
SNR	Signal-to-Noise Ratio
IMB	Intermediate Mass Binary
OSG	Open Science Grid
NSF	National Science Foundation

SUMMARY

The field of gravitational wave astronomy is a means of observing the universe in a new way. Crucial to the success of this new astronomy is analyzing the data obtained from the Laser Interferometer Gravitational-Wave Observatory (LIGO). Gravitational waves are oscillations of spacetime that propagate to Earth. We can predict these waveforms using solutions of Einstein's Equations from general relativity. There are several ways the LIGO scientific collaboration uses to detect signals. This thesis presents my work on one such method, Bayeswave analysis. Bayeswave analysis is one tool to process the data collected from the detectors. Bayeswave offers analysis on a potential event that is agnostic, in other words it is independent of theoretical predictions of the signal, due to it being a minimal assumption analysis and can be used to determine if the event is a signal, a glitch, or noise. Through the analysis, Bayeswave uses evidence values obtained from comparing signal, glitch, and noise models to determine what the event most likely is and produces reconstructions of both the signal and glitch models. This information can be used to further understand the event in the data. Although Bayeswave has shown to be able to accurately reconstruct simple waveforms, its ability to accurately reconstruct waveforms from systems with more complex initial parameters is not known. Therefore, this study is to determine if Bayeswave can accurately reconstruct known injected signals with varied initial parameter complexity. The ability for Bayeswave to reconstruct the more complex injected waveforms is gauged by analyzing the median overlap between the reconstruction and the injection as a function of signal-to-noise ratio (SNR), which is a gauge of how strong the signal is compared to

background noise, for various inclination angles, the strain and frequency data as functions of time, and the residual strain of the reconstruction waveform when it is subtracted from the injected waveform as a function of time.

CHAPTER 1

INTRODUCTION

The field of observational astronomy has been predominantly performed through the use of electromagnetic radiation from the universe. However, this constrains our knowledge to objects that emit electromagnetic radiation. Therefore, certain objects like black holes that do not directly emit electromagnetic radiation can only be observed indirectly by their impact on matter. Black holes are remnants of dead massive stars that have contracted down to an extremely density and compact body from which light cannot even escape its gravitational effects. Black holes can form binary system and these binaries are one of the targets of gravitational wave detection. Specifically, for this case study, binary black holes are the sources considered for the gravitational waves being analyzed. Gravitational waves are solutions to Einstein's Equations, however until recently they have only been predictions from the mathematics of general relativity. With the creation of the LIGO gravitational wave detectors by the National Science Foundation (NSF), the use of gravitational waves can now be employed as an observational tool to observe systems with compact objects, such as black holes and neutron stars. Further, they will reveal objects to which electromagnetic telescopes were blind, e.g. black holes.

There are currently two LIGO detectors, which function as large interferometers, with the Hanford detector stationed in Hanford, Washington and the Livingston detector stationed in Livingston, Louisiana. These detectors form a network that is able to detect gravitational waves by measuring the differential shift in the length of one of the arms of the interferometer compared to its rest length as a gravitational wave passes through the

detector. The gravitational wave perturbs spacetime which results in the length of the arm of the interferometer to vary slightly in a measurable way through interference patterns of lasers traversing both arms. The data corresponding to the interference pattern can be analyzed as a waveform signal. By reconstructing and analyzing the gravitational waveform signal, parameters about the system that generated them can be determined and thus a new astronomy is born. Shown in Figure 1., the first signal was detected on September 14, 2015, designated GW150914, which after much analysis, which included Bayeswave analysis, it was found that the signal was generated by a binary black hole system [2]. It was found that the initial black hole pair should have masses of around 36 solar masses and 29 solar masses, respectively, and the final black hole should have a mass of around 62 solar masses [2].

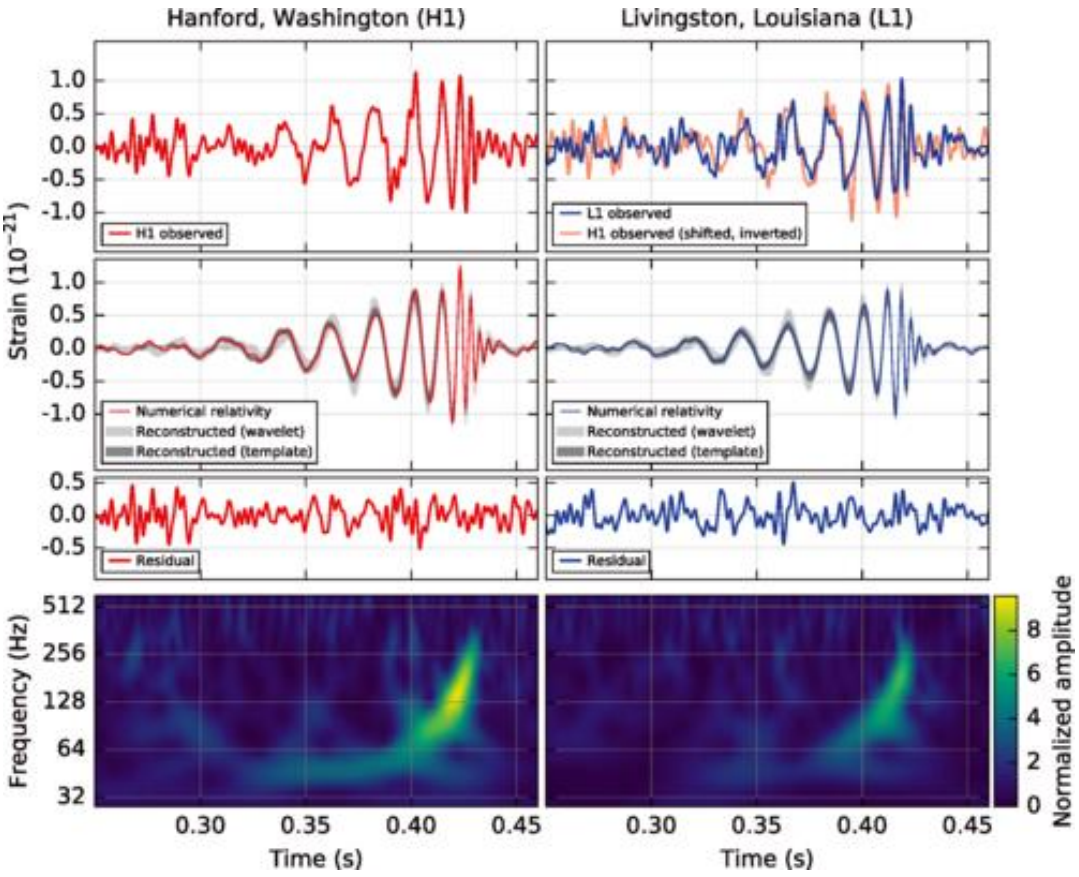

Figure 1. Gravitational signal data for GW150914 from the Hanford and Livingston detectors reprinted from [2]. This detection marked the beginning of gravitational wave astronomy, and displayed in the plot is the strain, residual strain, and frequency timeseries data which are all quantities being used in the analysis of this case study.

With the actual detection data shown in Figure 1., the diagram shown at the top of Figure 2. displays more information regarding the merger of binary black holes in general.

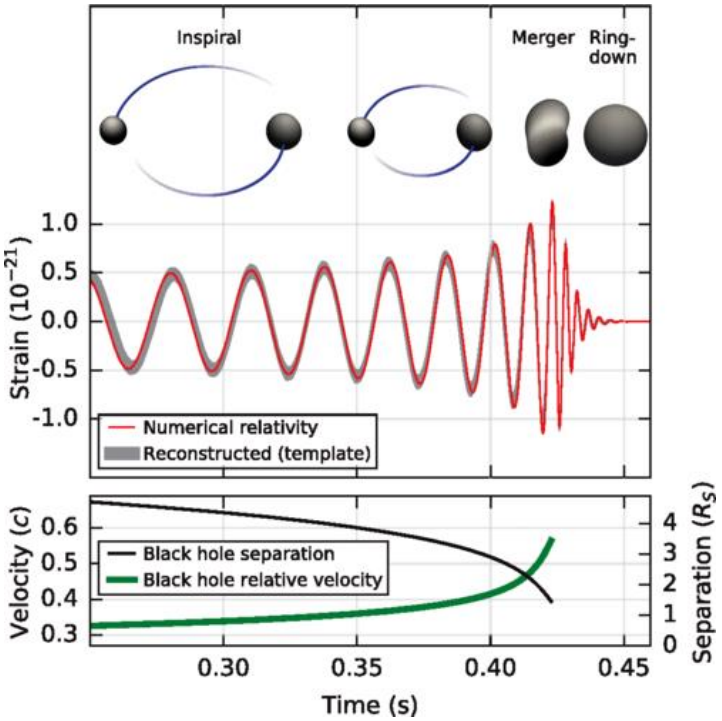

Figure 2. Diagram showing the stages of the merger over the corresponding section of the gravitational wave waveform reprinted from [2].

The diagram at the top of Figure 2. shows the various stages of a binary black hole merger with the three main stages labeled, such as the inspiral, merger, and ringdown. The inspiral is when the black holes are orbiting around one another as their orbits get smaller until they finally collide at the merger which is then followed by the ringdown period as the system settles down to a single black hole [2]. The stages of the coalescence of the black hole binary are positioned over the corresponding section of the gravitational radiation waveform produced by the system thus giving an idea of what each section of the waveform represents in regards to the physical system. With the GW150914 event, the first direct detection of gravitational waves as well as the first direct detection of binary black holes signaled the birth of new astronomy.

Model and Bayeswave Analysis

There are various methods employed to analyze and reconstruct the waveform signal. These methods include matched filter based on well-known models or a largely unmodelled minimal assumption search [4,5]. The matched filter approach can include models tuned to numerical relativity called equivalent-one-body (EOBNR) models and these models can be compared to the data to search for a signal [4]. EOBNR uses information from a post-Newtonian approximation for the inspiral data while the merger and ringdown is modeled with a superposition of the quasinormal modes of the final black hole [1]. However, the use of these models has the built-in assumption that the signal originated from a binary black hole system that satisfies Einstein's theory of gravity and/or a system that has been completely modeled, which might not always be the case [4]. An unmodelled search relies on no such assumptions, but is only useful for strong signals, i.e. those with high SNR.

One such tool is Bayeswave analysis which is done following a trigger, which is a cluster of time-frequency data that has a power greater than that of the background noise present in both detectors, in the coherent wave burst (cWB) pipeline, which bases the detection of a signal on correlations between the data in both detectors [3]. With the cWB pipeline, the data is analyzed coherently between the two detectors to see if there is any sign of a trigger [3]. If a trigger was only found in one detector it could be a glitch since if there is a signal evidence of it should be seen in both detectors. Since Bayeswave is considered a burst search, a trigger in this case would be a short duration transient in the data which are known as gravitational-wave bursts [3]. Bayeswave analysis does not assume there is a signal, but rather accounts for a signal and glitch model for the data to

determine if the evidence supporting the event in the data is a signal or a glitch [6]. Glitches are the designation given to artifacts in the data that result from the non-Gaussian noise transients in the data and thus are not true astrophysical signals [6]. Bayeswave creates the reconstructions for both a signal and glitch waveform based on using different combinations of wavelets as well as the posterior distributions for the wavelet parameters [6].

Effectiveness of Bayeswave

Even though the results obtained by the modeled searches and Bayeswave analysis are consistent within statistical uncertainty when tested using the GW150914 event, Bayeswave is perhaps a more effective tool in analyzing the detector data [4]. This is due to the fact that it makes minimal assumptions on the incoming signal as well as helps discern between glitches and signals even at high signal-to noise ratios, which has been problematic in the past [4,9]. Signal-to-noise ratios (SNR) is a measure of how prominent the signal is compared to the noise of the data and is thus a gauge of how strong or "loud" the signal is compared to the noise in the data.

However, even though Bayeswave has been shown to recover the waveform of simple waveform signal injections, it is not known whether it is able to recover more complex waveforms. For comparison, GW150914 would be considered a simple signal from the consideration of system parameters for this study since the black holes were largely equal in mass within the stated error bars [2]. Therefore, the purpose of this study is to determine the effectiveness of Bayeswave analysis to recover more complex waveform signal injections. This would prove that it would be able to discern simple signals from complex signals from detector data by analyzing the reconstruction data for

signal injections that vary in parameters including: inclination angle, SNR, and mass ratio.

The inclination angle is the measure of how inclined the plane of the black hole system is as seen from Earth with 0° defined as looking directly at the plane of the system, called “face-on”, and with 90° defined as looking at the edge of the plane of the system, called “edge-on”. Mass ratio is determined to be the ratio of the masses of the two black holes, such as a mass ratio of 5 corresponds to one of the black holes being 5 times the mass of the other while a mass ratio of 1 corresponds to the two black holes having equal masses.

CHAPTER 2

LITERATURE REVIEW

In the field of gravitational wave astronomy, it is of great importance to have accurate models and analysis processes in place so as to obtain the best estimate about the parameters of the system that produced a signal. Ground based detectors, such as LIGO, can be noisy due to seismic, photon shock, and other noise sources on Earth, so accurate models allow us to detect the weakest signals that we could not have seen otherwise [2]. Once data is obtained through the LIGO detectors, it goes through data pipelines where the data is processed to determine if there is indeed an event. Burst searches specifically look for short duration transients in the detector data, such as the signal event GW150914 [3]. The two main pipelines that are employed for burst search analysis are omicron-LALInference-Bursts (oLIB), which is designed for low latency, and cWB, which looks for correlations in the data between the detectors without considering a signal being present [3]. Following the identification of a trigger in the cWB pipeline, a BayesWave analysis is performed to reconstruct the data for both a glitch and signal model [3,9]. The Bayeswave Analysis is important because it confirms that the analysis results for the event is not biased by models.

Data Pipelines

When an event trigger is found in the cWB pipeline it is classified into one of three groups, C1, C2, or C3 depending on its time-frequency morphology [3]. Events that are characterized as a “blip glitch”, which is a noise transient of unknown origin with few cycles around 100 Hz, or a glitch due to narrow-band features, which has most of its

energy within a frequency band width of 5 Hz, are placed in C1 [3]. Events that express a frequency increasing with time and residual energy consistent with Gaussian noise are placed in C3 [3]. All other events are placed in C2 [3]. With the glitches contained in C1, the sensitivity of detecting a signal in C2 and C3 are increased [3].

The analysis in the oLIB pipeline begins with a time-frequency map of the single-interferometer strain data from each detector being produced and stretches of excess power are marked as triggers [3]. All coincident triggers marked in the data are analyzed using a Bayesian parameter estimation and model selection algorithm that coherently explores the signal parameter space [3]. Glitches and signals are modeled using a single sine-Gaussian wavelet where signals have a coherent phase across detectors whereas glitches do not [3]. With these models, a Bayes factor for coherent signal vs Gaussian noise and a Bayes factor for coherent signal vs incoherent glitch are computed each of which is an evidence ratio between the two hypotheses being considered [3]. The two Bayes Factors are then combined to form a scalar likelihood ratio [3]. These scalar likelihood ratios are then evaluated for a different set of background triggers from time-shifted data to map a certain value of the likelihood ratio into a false alarm rate for signals [3].

Bayeswave Pipeline and Model Searches

The Bayeswave pipeline acts as a follow up to triggers marked in the cWB pipeline and analyzes the data with a Bayesian algorithm designed to robustly distinguish gravitational wave signals from glitches in detector data [3]. For each potential event in the data, the marginalized likelihood, or evidence, is compared between three hypotheses: the data only contains Gaussian noise, the data contains a glitch, or noise transient, and Gaussian noise, and the data contains an astrophysical signal and Gaussian noise [3].

Bayeswave models signals and glitches through linear combinations of sine-Gaussians with the optimal number being needed determined from a reversible jump Markov chain Monte Carlo [3,6]. The glitch model fits data separately in each detector, whereas the signal model reconstructs the event in the data based on the response of each detector in the network for that signal [3]. Bayeswave generates posterior distributions for the parameters of each model, and the marginalized posterior, or evidence, for each model is computed by marginalizing over the different dimension waveform reconstructions for each model which is used to rank the three hypotheses being considered [3,5]. The effectiveness of Bayeswave with regards to the use of Bayes factors has been shown to be a useful tool through its good fit with the data from the LIGO detectors from the sixth LIGO science run [9].

Along with the pipeline searches for events in the data, there are also other model searches that specifically search for binary coalesces. One such prominent model that is used is EOBNR as aforementioned [4]. However, these models are based on the idea that the signal in the data originates from a binary system which puts restrictions on what the data can identify with these methods [4]. Thus, if the source was a non-binary system or if physics is missing in the models then the analysis from these models could give inconsistent results. Therefore, a minimal assumption search would be a better approach at trying to identify a general signal from the detector data. Bayeswave is a minimal assumption analysis since it does not assume anything about the signal or that the data even contains a signal [4]. Therefore, Bayeswave could function as a more efficient tool, in general, for determining the presence of a signal in the data and thus the parameters

that could be reconstructed for the source that produced the signal once a signal was identified.

Bayeswave Reconstruction Complexity

Although Bayeswave is able to recover simple waveform signal injections well, it has not been validated for complex waveforms. Increased complexity in this case is deviations from an equal mass, face-on system in that the mass ratio and inclination angle, both of which will add amplitude and phase modulations to the waveform, are varied. We also need to validate with and without the presence of background noise, however for this current study only injections without noise are used.

The variations in the parameters for the initial waveform injections should affect the morphology of the reconstructed waveform generated by Bayeswave and can be compared to the original waveform injection to determine if the morphology was recovered correctly. One way to gauge signal complexity is through looking at the Bayes factor that compares the signal and glitch models from Bayeswave analysis [3]. Therefore, these Bayes factors could potentially be used as a means to express the complexity of the waveform injection that is being reconstructed [3].

However, the method that is being employed in this current study of Bayeswave's ability to recover complex waveform injections is through both quantitative as well as qualitative gauges. The quantitative gauge is analyzing the median overlap and how it varies as a function SNR since the median overlap is a specific quantity that expresses how well the reconstructions match with the injection waveforms. The qualitative gauges are generating plot for the strain and frequency timeseries of the reconstructions and the injection waveforms as well as the residual strain timeseries, which is what remains once the injection waveform is subtracted from the reconstruction waveform.

The median overlap will give a numerical overall comparison of the reconstruction and injection waveforms while the strain, frequency, and residual strain timeseries plots will allow for localizing discrepancies between the reconstruction and injection waveforms. Combining these complexity gauges will provide a more comprehensive analysis as to the accuracy of the ability for the Bayeswave reconstructions to recover the complexity of the injection waveforms. This study will potentially demonstrate that Bayeswave is not only effective at recovering simple waveform injections, but also more complex waveform injections as well.

CHAPTER 3

METHODOLOGY

For this study, the accuracy of the Bayeswave reconstructions to recover a given injected waveform with varying complexity is gauged through analyzing the overlap between an injected waveform and its reconstruction. Specifically, the strain and frequency data as a function of time for the reconstruction and injection waveforms, and the residual strain data as a function of time. The injected waveform is produced with an EOBNR model which treats the two-body problem of the binary black hole system as an effective one body system with corrections provided by numerical relativity [1]. The EOBNR injection waveforms are generated with various initial parameters to vary their complexity. The injections are then processed through Bayeswave analysis to produce the reconstruction waveforms. This reconstruction data is being employed by the methods aforementioned to determine if the complexity in the injection waveform is being recovered by the reconstruction.

EOBNR Injections

The EOBNR waveform injection files are generated using lalapps_inspinj which produces a sim-inspiral table which is saved as a .xml file format[1]. The EOBNR model

[1] The code for generating the sim-inspiral tables can be found here https://github.com/bday336/Bayeswave-Complexity-Study/blob/master/gen_xml_HM.sh

that is used is EOBNRv2HMpseudoFourPN, which is an EOBNR model that includes higher order modes in the waveforms it generates. Higher order modes of the waveform can be considered overtones in frequency or higher order spherical harmonics for the waveform signal. The data requires a gpsstart time to base the analysis on which can arbitrarily be chosen. For this study, the gpsstart time is given to be 1150569646.

The physical parameters of the injection waveforms are specified to mimic a signal. The total mass of the system must also be set and has been chosen to be 100 solar masses for this study. This total mass value was chosen since it is situated in the lower bound of the region for Intermediate Mass Binaries (IMBs) to be detected. In this region of parameter space burst searches become competitive with match filtering searches, which are searches that use waveform templates to attempt to extract the parameters of the system that produced the signal by relating it to numerical relativity simulation waveforms. The mass ratios, typically denoted by the symbol $q = m_1/m_2 \geq 1$, being tested in this case study are 1, which indicates that the two black holes in the simulated injection are equal mass, and 5, which indicates that the one of the two black holes is five times the mass of the other. The waveforms corresponding to mass ratio 1 are considered the control group since they are simpler systems and should be recovered well by Bayeswave while the waveforms corresponding to mass ratio 5 are considered the test group since they are more complex systems and will be a more definitive gauge on the ability of Bayeswave to recover increased waveform complexity.

For each injection file, it is given a mass ratio, an SNR value, and an inclination angle, which is the measure of how inclined the plane of the black hole system is as seen from Earth with 0° defined as looking directly at the plane of the system, called “face-

on", and with 90° defined as looking at the edge of the plane of the system, called "edge-on". The inclination angles used in this study span from 0° to 360° in increments of 45°. For each inclination angle value, the value of SNR is varied from 10 to 50 in increments of 10. Therefore, there are forty-five injection files corresponding to each mass ratio value tested due to the total combination of inclination and SNR values.

Setup Run Directories

For each of the injection files, a script called bwb_pipe.py must be called with the argument corresponding to the configuration file for that injection file. However, in the script that calls bwb_pipe.py the tag "—sim-data" must be included for it to recognize the simulation data[2,3]. The configuration file contains the paths to the necessary scripts that will need to be called from the run directory, which is generated from the bwb_pipe.py script, as well as the parameters for the Bayeswave analysis, such as including no noise in the main analysis and/or the post-processing stages[4]. The argument of the bwb_pipe.py script call will be the name of the run directory that is generated.

Each run directory contains 100 waveform directories that are ready for Bayeswave analysis to be performed on them and these waveforms vary in that they are given random sky localizations while holding all other parameters constant. While the sky localizations are random for a given waveformin a run directory, all the waveforms in

[2] The script to call bwb_pipe.py can be found here https://github.com/bday336/Bayeswave-Complexity-Study/blob/master/run_pipe.sh
[3] The code for bwb_pipe.py can be found here https://github.com/astroclark/osg_tools/blob/master/bwb/bin/bwb_pipe.py
[4] A sample configuration file for running on a local machine can be found here https://github.com/bday336/Bayeswave-Complexity-Study/blob/master/q_1_inc_0_snr_10.ini

each run directory generated will have the same set of random waveforms. While in the run directory of the injection that Bayeswave analysis is to be performed on, the user needs to enter the command "condor_submit_dag *dag" which will submit the .dag file in the run directory to condor for job distribution on the computer that is being currently used. The analysis time will vary depending on the computing resources on the computer. The control group of runs, which are the equal mass (q=1) waveforms, were analyzed using a single machine and thus took a long time to complete. However, the test group of runs, which are the unequal mass (q=5) waveforms, were analyzed using condor job distribution through the Open Science Grid (OSG)[5]. The OSG is a system of connected machines throughout the country which allows computational jobs to be outsourced thus making it possible to run many more at once than would be possible on a single machine. The use of the OSG allows the analysis of the test group of waveforms to be done much quicker thus expediting the data collection process.

The analysis populates the files in the waveform directory with the data corresponding to each and includes data for both the Hanford and Livingston detectors. The data from the analysis contains the strain timeseries for the reconstruction and injection waveforms as well as the frequency timeseries for the reconstruction waveforms. The data corresponding to the frequency timeseries for the injection waveform had to be produced separately using an independent script which is run in the

---

[5] A sample configuration file for running on the OSG can be found here https://github.com/bday336/Bayeswave-Complexity-Study/blob/master/config_OSG.ini and a sample script to call bwb_pipe.py with the appropriate OSG flags can be found herehttps://github.com/bday336/Bayeswave-Complexity-Study/blob/master/run_bwb-pipe.sh

same directory as the strain data for the injection waveform[6]. The injection waveform data has data corresponding to each detector that is processed through Bayeswave. Thus, there is also a reconstructed waveform for each detector.

Data Processing and Plots

With the Bayeswave analysis completed for all SNR values for all inclination angle sets, the data can be processed and plotted to be used to gauge if the reconstruction accurately recovered the injected waveform. The data in this study will be considered for both of the detectors individually. Therefore, there will be separate plots for the data relating to the Hanford detector and the data relating to the Livingston detector. The accuracy of the Bayeswave reconstruction to recover the complexity of the injection waveform is gauged in this study by considering median overlap, the structure of the strain and frequency of the reconstruction as functions of time compared to the injection waveform, and the amount of residual strain as a function of time remaining when the injection strain data is subtracted from the reconstruction strain data.

Median Overlap

The median overlap is a gauge of how much the injection waveform matches with the reconstructed waveform. The overlap is calculated by taking the dot product of the injection data and the reconstruction data which is then divided by both the magnitude of

---

[6] The configuration script to generate the frequency timeseries data for the injection waveform can be found here https://github.com/bday336/Bayeswave-Complexity-Study/blob/master/bayeswave_tftrack.cand the makefile can be found here https://github.com/bday336/Bayeswave-Complexity-Study/blob/master/Makefile

the injection data and the magnitude of the reconstruction data. To compute the scalar product the data must be converted from a function of time to a function of frequency using a Fourier transformation. However, since the data is discrete a discretized form of the Fourier transform must be used which is given in Equation 1.

$$\tilde{h}_k(f) = \frac{1}{N}\sum_{n=0}^{N-1} h_n(t) e^{\frac{i2\pi nk}{N}} \quad (1)$$

Where ˜h_k(f) is the k^{th} value of the data in the function domain, N is the total number of data samples present in the data, h_n(t) is the n^{th} value of the data in the time domain [7]. The scalar product is given by Equation 2.

$$\langle I|R\rangle = 2\int_0^{\infty} \frac{\tilde{I}(f)\tilde{R}^*(f) + \tilde{I}^*(f)\tilde{R}(f)}{Sn(f)}\, df \quad (2)$$

where ˜I(f) is the injection data as a function of frequency which is a complex number and its complex conjugate is ˜I*(f), ˜R(f) is the reconstruction data as a function of frequency which is a complex number and its complex conjugate is ˜R(f), and Sn(f) is the spectral density of the noise in the detector which constitutes weights for the integral [8]. To determine how well the data between the injection and the reconstruction overlap, or match, with each other, an overlap between them is performed as shown in Equation 3.

$$Overlap(I|R) = \frac{\langle I|R\rangle}{\sqrt{\langle I|I\rangle}\sqrt{\langle R|R\rangle}} \quad (3)$$

where I is the injection waveform data and R is the reconstruction data. To compute the overlap, the scalar product is employed once the data has been converted from a function of time to a function of frequency. An overlap of 1 indicates a perfect match between the injection and reconstruction data while an overlap of 0 indicates a perfect mismatch between the injection and reconstruction data.

For each waveform directory in the run directory for a given set of parameters, the network overlap data is stored in the "post" directory of the specific waveform directory in the file "signal_whitened_moments.dat.0" for the data relating to the Hanford detector and "signal_whitened_moments.dat.1" for the data relating to the Livingston detector. With the network overlap data extracted, the median of the data set is found and plotted as a function of SNR for each specific waveform[7]. The plot in Figure 3. shows a sample plot of median overlap as a function of SNR data from the Hanford detector for the waveform bayeswave_1150569652.368886232_0.0 for all the inclination sets corresponding to the control group with the black holes having equal masses (q=1). The error bars represent one standard deviation from the median overlap of the one hundred overlaps values produced from the one hundred waveform reconstructions produced for this specific waveform injection. A plot in Figure 3. shows a sample plot of the median overlap data as a function of SNR for all inclinations tested for the Hanford detector corresponding to the waveform bayeswave_1150569652.368886232_0.0 for each set of parameter values.

---

[7] The code used to generate these plots can be found here https://github.com/bday336/Bayeswave-Complexity-Study/blob/master/med_overlap.py

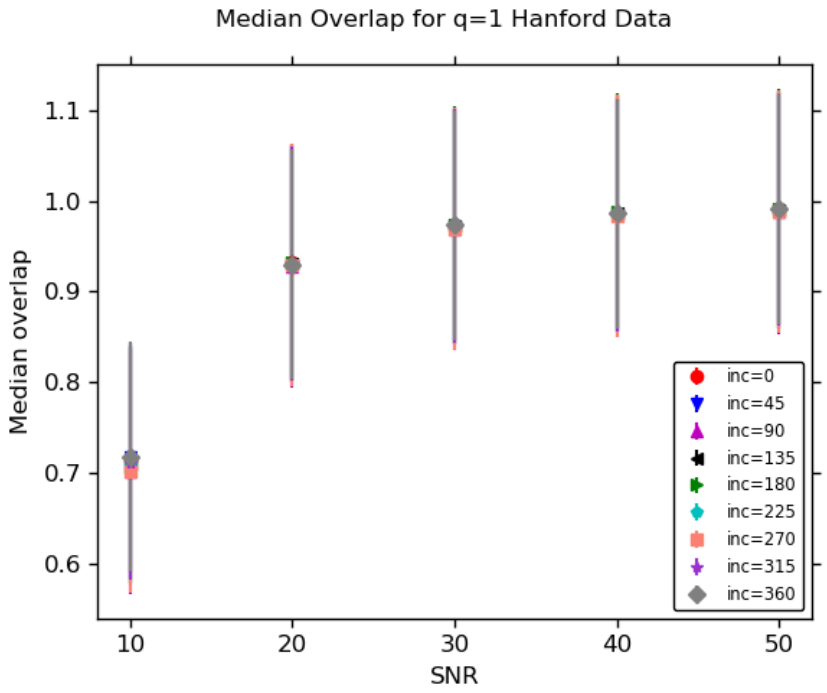

Figure 3. Median overlap with error bars as function of SNR for Hanford data for all inclination angles tested.

By comparing how the median overlap as a function of SNR varies with inclination angle, the accuracy of the reconstruction can be gauged for the inclination angles being considered for various SNR values.

Strain and Frequency Timeseries

The LIGO detectors function as a large interferometer and measure gravitational waves as they pass through the detector in that the gravitational wave will slightly perturb spacetime around the detector. This will either shorten or elongate one of the arms of the detector in a predictable way calculated through general relativity. The differential change in the arms of the LIGO interferometer detector is called strain.

For the EOBNR injections being used, the strain is in geometrized units and can be used to measure the oscillations in the gravitational wave. The strain has both a real

and imaginary component. However, for the purpose of this study only the real component of the injection and reconstruction strain data are being plotted in consideration of how accurately they resemble each other. For each waveform directory in the run directory for a given set of parameters, the reconstruction strain data as a function of time is stored in the "post" directory of the specific waveform directory in the file "signal_median_time_domain_waveform.dat.0" for the data relating to the Hanford detector and "signal_median_time_domain_waveform.dat.1" for the data relating to the Livingston detector. Also, the injection waveform strain data as a function of time is stored in the "post" directory of the specific waveform directory in the file "injected_whitened_waveform.dat.0" for the data relating to the Hanford detector and "injected_whitened_waveform.dat.1" for the data relating to the Livingston detector.

Along with the strain, the frequency data of the reconstruction is plotted as a function of time. Since gravitational waves have a real and imaginary component, the strain can be considered like a vector in the complex plan which can be described as having a magnitude relating to the magnitude of the strain and a phase angle defined from the positive real axis. The frequency considered in this study is the time derivative of this phase angle which corresponds to the frequency of oscillations for the strain data.

For each waveform directory in the run directory for a given set of parameters, the reconstruction frequency data as a function of time is stored in the "post" directory of the specific waveform directory in the file "signal_median_tf.dat.0" in the "post" directory for the data relating to the Hanford detector and "signal_median_tf.dat.1" in the "post" directory for the data relating to the Livingston detector. Once the separate script is run to generate the injection frequency timeseries data, the data can be found in

"injected_median_tf.dat.0" in the "post" directory for the data relating to the Hanford detector and "injected_median_tf.dat.1" in the "post" directory for the data relating to the Livingston detector. Both the strain and frequency of each waveform is extracted and plotted as a function of time to see how the waveform reconstruction data looks[8]. The plot in Figure 4. shows a sample plot of the strain and frequency data as functions of time for the Hanford detector for the waveform bayeswave_1150569652.368886232_0.0.

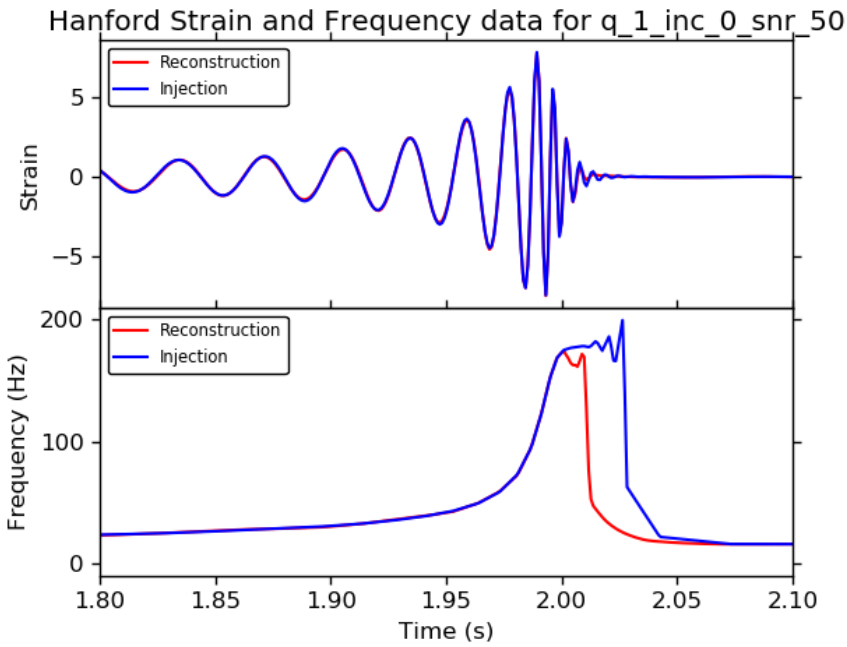

Figure 4. Strain and frequency data as functions of time for the Hanford detector. Waveform has parameters: mass ratio=1, inclination=0°, and SNR=50.

By comparing the strain and frequency of the waveform reconstruction, it can be seen how well the injection and reconstruction data directly compare to one another. Thus, it

[8] The code used to generate these plots can be found here https://github.com/bday336/Bayeswave-Complexity-Study/blob/master/strain_freq_residual.py. This script is used to generate the strain and frequency plots as well as residual strain plots for both the control and the test group.

can be used as a qualitative gauge on how much the reconstruction resembles the injected waveform and if there are any very obvious issues with the reconstruction data.

Residual Strain Timeseries

Since the study is attempting to prove how well the Bayeswave reconstructions correspond with the injected waveform, a useful tool can be to find the residual strain of the waveforms. The residual strain is found from subtracting the injected waveform strain as a function of time from the reconstruction waveform strain as a function of time. This will give a gauge as to how different the two waveforms are and where the main differences are located in the timeseries data. If the injection was the same as the reconstruction it would be expected that the residual strain data would be zero for each data sample for the timeseries, therefore any non-zero regions of residual strain indicated differences in the injection and reconstruction waveforms.

The strain data for the reconstruction and injection waveforms is the same strain data used in the strain and frequency timeseries plots[9]. The plot in Figure 5. shows a sample plot of the residual strain as a function of time from the Hanford detector for the waveform bayeswave_1150569652.368886232_0.0.

[9] The code used to generate these plots can be found here https://github.com/bday336/Bayeswave-Complexity-Study/blob/master/strain_freq_residual.py. This script is used to generate the strain and frequency plots as well as residual strain plots for both the control and the test group.

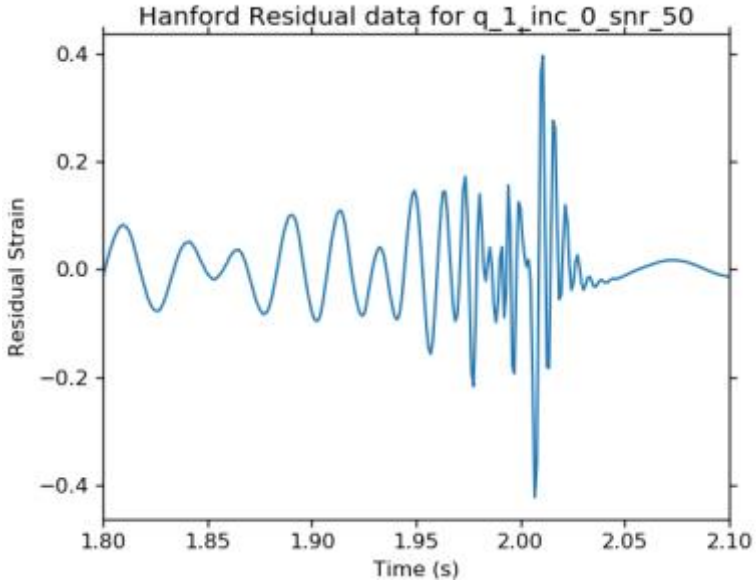

Figure 5. Residual strain data as a function of time for the Hanford detector. Waveform has parameters: mass ratio=1, inclination=0°, and SNR=50.

Through using the residual strain data, it can be determined where the reconstruction best corresponds with the injection as well as if there are any localized regions in the data where the two seem to be quite difference. Any localized difference would show a noticeable amount of residual since they would not cancel each other as much as the other regions in the data.

CHAPTER 4

RESULTS

The results for the control group and test group of injections which make up the set of trials where the mass ratio is 1 and 5, respectively, are presented here for this case study. For the case study analysis only a single sky localization, which has the label waveform bayeswave_1150569652.368886232_0.0, is being analyzed out of the one hundred random sky localization that are undergoing the Bayeswave analysis for each set of parameter values. The analysis for the other ninety-nine will potentially be used in follow up studies to average the results over sky localization. Since the data is largely similar between the two detectors, the Hanford detector data is highlighted to represent the trends observed for both detectors. The data is presented below for median overlap, strain and frequency timeseries, and residual strain timeseries.

Control Group

The data collected for the control group corresponds to the data set of all the waveform injections that have a mass ratio of one. This is used as a control group since equal mass systems are largely simple systems that Bayeswave analysis has already been shown to recover accurately.

Median Overlap

The data presented here for median overlap has been collected for both detectors for all SNR values tested, which include 10, 20, 30, 40, and 50, for all inclination angles tested, which include 0, 45, 90, 135, 180, 225, 270, 315, and 360 degrees. For each detector, all the median overlap data with corresponding error bars is presented in a

single plot showing the trend of median overlap as a function of SNR for each inclination angle and is shown in Figure 6. for the Hanford detector and in Figure 7. for the Livingston detector. The Livingston detector data is presented here for completeness for median overlap data for the control group.

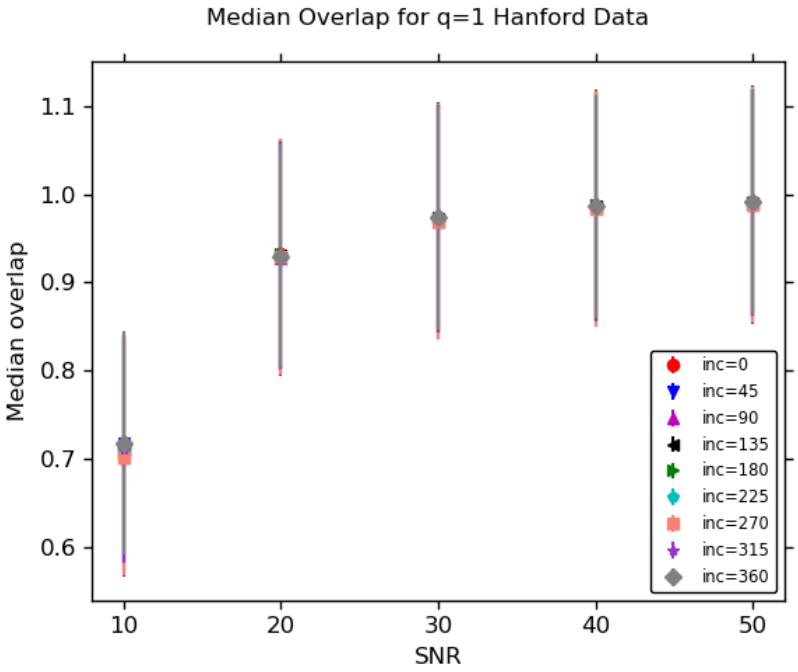

Figure 6. Median Overlap for Hanford detector for Control Group

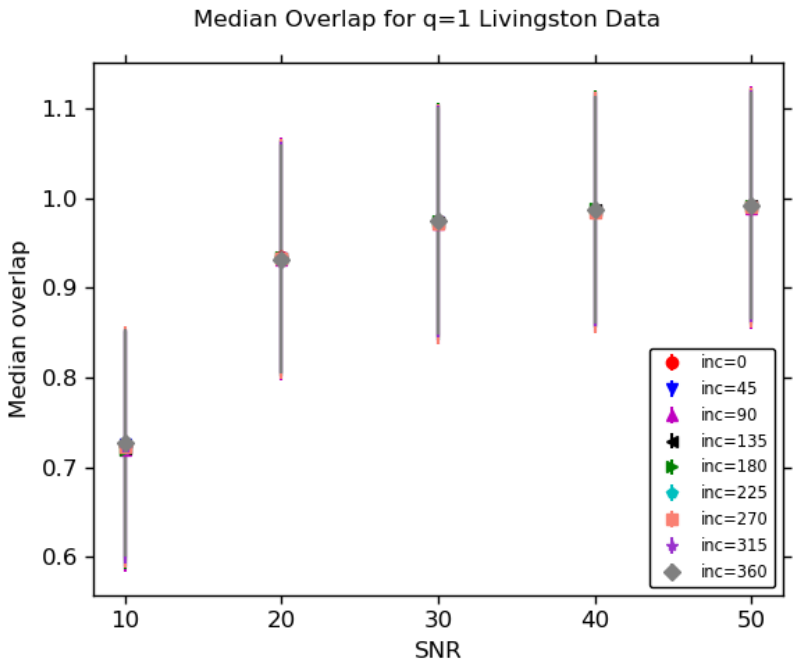

Figure 7. Median Overlap for Livingston detector for Control group

The median overlap data represents the median network overlap value with respect to the original injection waveform for the one hundred reconstructions that are produced from Bayeswave analysis for the original injection waveform. Thus, it gives a quantitative value for comparing the reconstructions and the injection waveforms. The trend in the median overlap as a function of SNR shows that the reconstruction waveform recovers more and more of the injection waveform with increasing SNR, which would be expected since with higher SNR the more prominent the injected signal and thus Bayeswave has a better chance of recovering it more completely. This trend is observed for all inclination angles with all values being close on the plot thus inclination angle does not seem to affect Bayeswave's ability to recover the injection waveform.

Strain and Frequency Timeseries

The data presented here is for the strain and frequency timeseries collected for all SNR values tested, which include 10, 20, 30, 40, and 50, for all inclination angles, which

include 0, 45, 90, 135, 180, 225, 270, 315, and 360 degrees. The data can largely be summarized by presenting plots for a single inclination value since the median overlap plots in the previous section show that inclination does not affect the effectiveness of the Bayeswave reconstruction. Also, the data for an SNR of 10 and 50 waveform were considered here to give a comparison of how Bayeswave is more accurate with higher SNR.

During the analysis of the plots, it was found that there were interesting localizations of error between the reconstructions and injection waveforms in the inspiral and ringdown sections of the data. Therefore, two sets of plots were produced to include the different regions of interest better. The first set of plots include the inspiral region, which will be referred to as the inspiral plots, while the second set focuses more on the merger-ringdown region, which will be referred to as the ringdown plots. The Hanford data strain and frequency plots for inclination angle of 45 degrees for both SNR 10 and 50 for the inspiral plots are shown in Figure 8. and Figure 9., respectively.

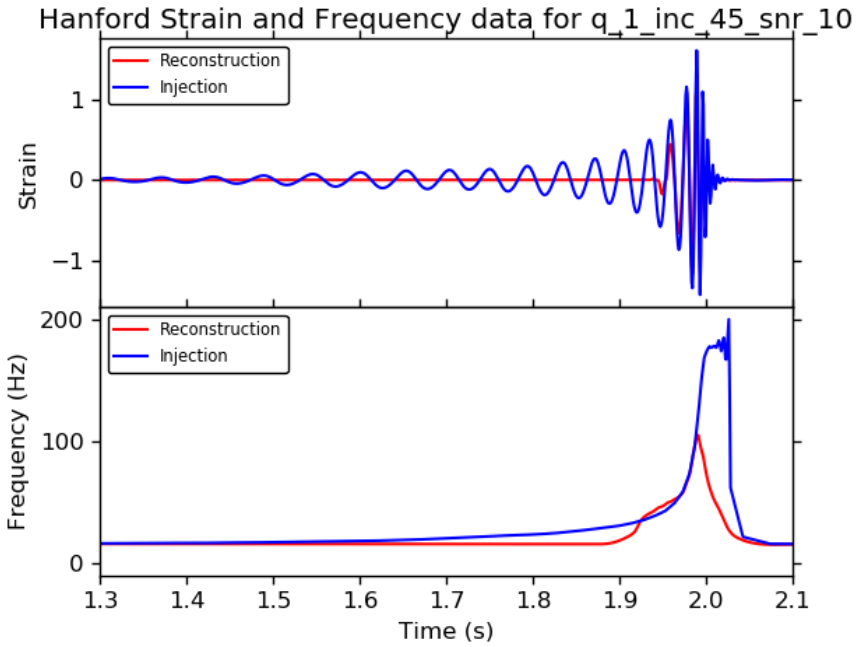

Figure 8. Inspiral plot for the Hanford detector. Waveform has parameters: mass ratio=1, inclination=45°, and SNR=10.

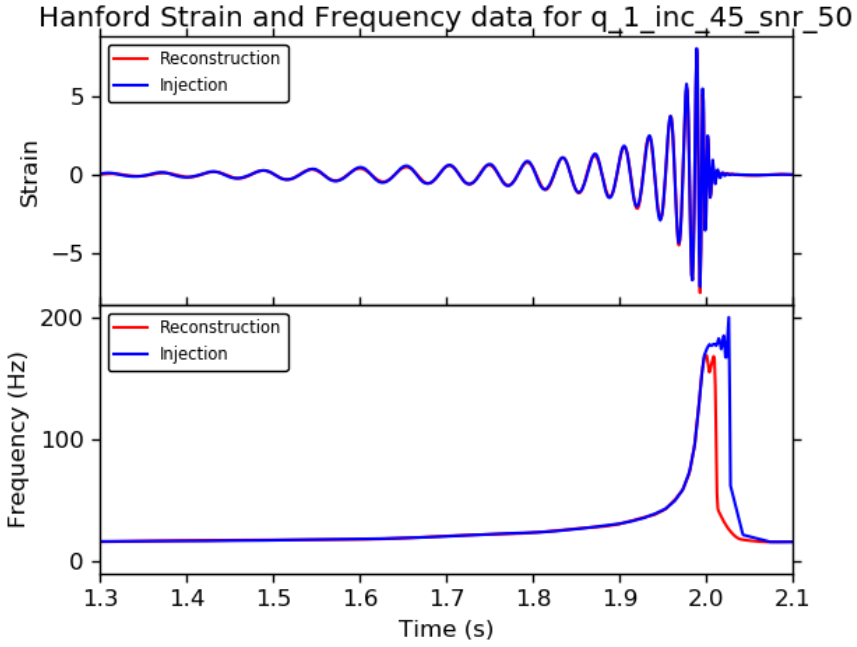

Figure 9. Inspiral plot for the Hanford detector. Waveform has parameters: mass ratio=1, inclination=45°, and SNR=50.

The inspiral plots allow for a more complete view of the waveforms so as to see how well the reconstruction recovers the injection waveform. It is found that the injection

waveforms with a low SNR, such as 10, are recovered poorly compared to the injection with a high SNR, such as 50. Thus, reconstructions for higher SNR value injections would be a better gauge for Bayeswave's ability to recover the waveform as would be expected. It is also interesting to note that there are no obvious amplitude modulations present in the strain nor frequency data rather it expresses an increasing trend before the merger and decreasing trend after the merger.

The ringdown plots for the Hanford data strain and frequency plots corresponding to a waveform with an inclination angle of 45 degrees for both SNR 10 and 50 are shown in Figure 10. and Figure 11., respectively.

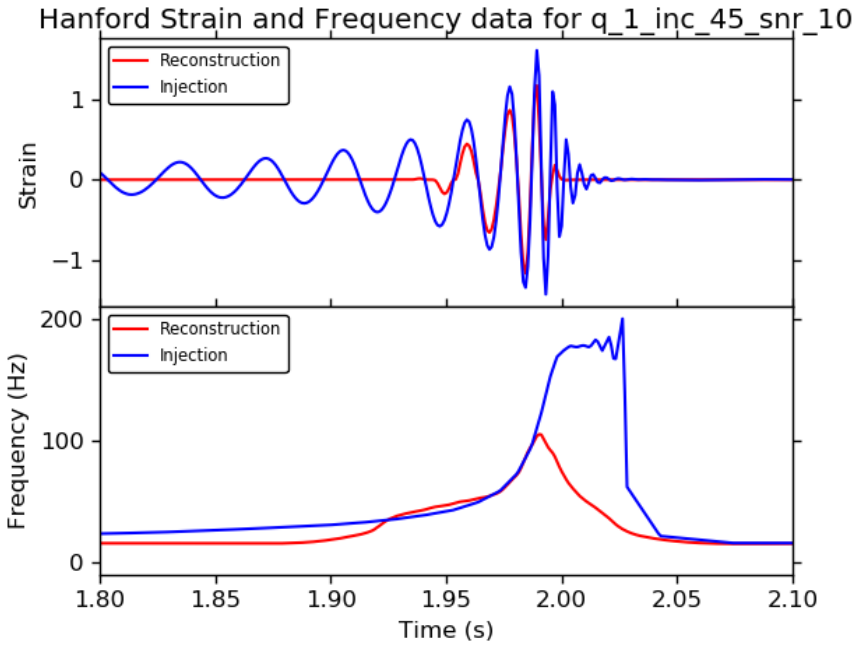

Figure 10. Ringdown plot for the Hanford detector. Waveform has parameters: mass ratio=1, inclination=45°, and SNR=10.

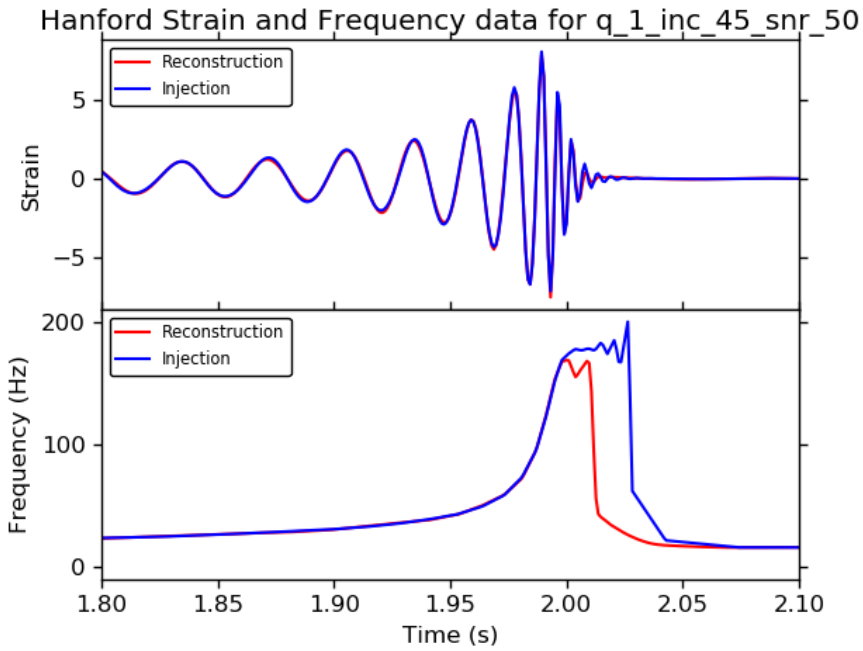

Figure 11. Ringdown plot for the Hanford detector. Waveform has parameters: mass ratio=1, inclination=45°, and SNR=50.

The ringdown plots allow for a more complete view of the waveforms specifically in the region around the merger and ringdown phases of the binary black hole merger. While the strain for the SNR 10 wave is recovered poorly, there is not much of a noticeable discrepancy in the strain timeseries for the SNR 50 reconstruction. However, there is a very noticeable discrepancy in the frequency timeseries plots, so there is an issue with the recovery of the ringdown region of the injection waveform for both SNR values. As with the inspiral plots, the higher the injection SNR the better the reconstruction recovers the injection waveform which would be expected since Bayeswave is effective at higher SNR [9]

Residual Strain Timeseries

The data presented here is for the residual strain collected for all SNR values tested, which include 10, 20, 30, 40, and 50, for all inclination angles, which include 0,

45, 90, 135, 180, 225, 270, 315, and 360 degrees. The data can largely be summarized by presenting plots for a single inclination value since the median overlap plots in the previous section show that inclination does not affect the effectiveness of the Bayeswave reconstruction. Also, as well the strain and frequency plots, the data for an SNR of 10 and 50 waveform were considered here to give a comparison of how Bayeswave is more accurate with higher SNR.

As with the strain and frequency plots, the residual strain plots were generated in two sets for the two regions of interests that were found, namely the inspiral and merger-ringdown sections of the waveforms. The inspiral plots for the Hanford residual strain timeseries data corresponding to sets of an inclination angle of 45 degrees and SNR values of 10 and 50 are shown in Figure 12. and Figure 13., respectively.

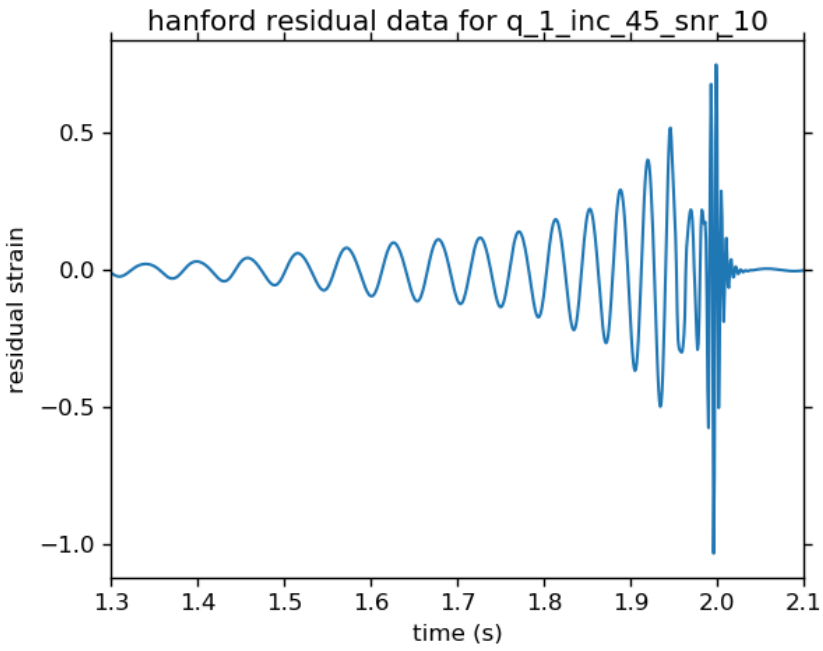

Figure 12. Inspiral plot for the Hanford detector. Waveform has parameters: mass ratio=1, inclination=45°, and SNR=10.

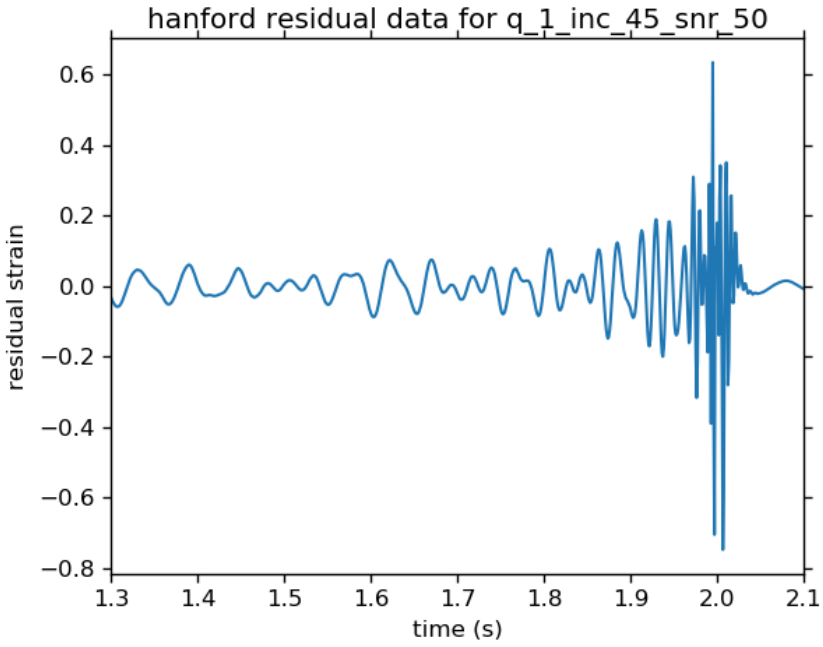

Figure 13. Inspiral plot for the Hanford detector. Waveform has parameters: mass ratio=1, inclination=45°, and SNR=50.

As with the inspiral plots for the strain and frequency, the residual strain inspiral plots express a more complete view of how well the reconstruction compares with the injection waveform. The residual strain plots are perhaps more telling in that for the reconstruction and injection waveform to be rather similar the residual strain should be almost zero for each time value. The residual strain plots for the waveforms corresponding to low SNR values there is come structure to the residual data whereas it is not seen except for around the merger-ringdown region of the waveform for waveforms corresponding to higher SNR values. The inspiral plots for the residual strain thus express the same as the strain and frequency plots that the correspondence between the injection and reconstruction waveforms increases with SNR value, but does not seem to be effected much by inclination angle.

The ringdown plots of Hanford residual strain data corresponding to an injection waveform with an inclination angle of 45 degrees for both SNR values are shown in Figure 14. and Figure 15., respectively.

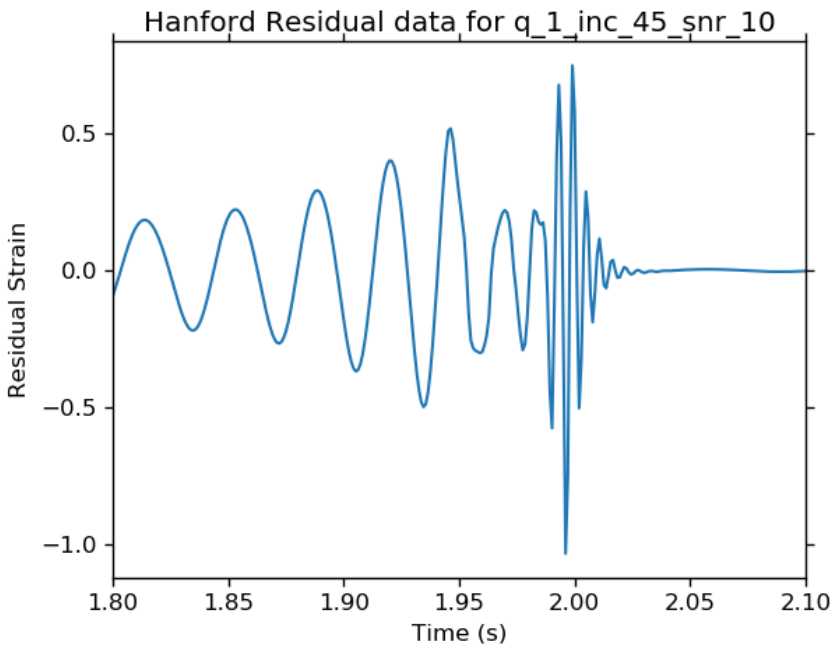

Figure 14. Ringdown plot for the Hanford detector. Waveform has parameters: mass ratio=1, inclination=45°, and SNR=10.

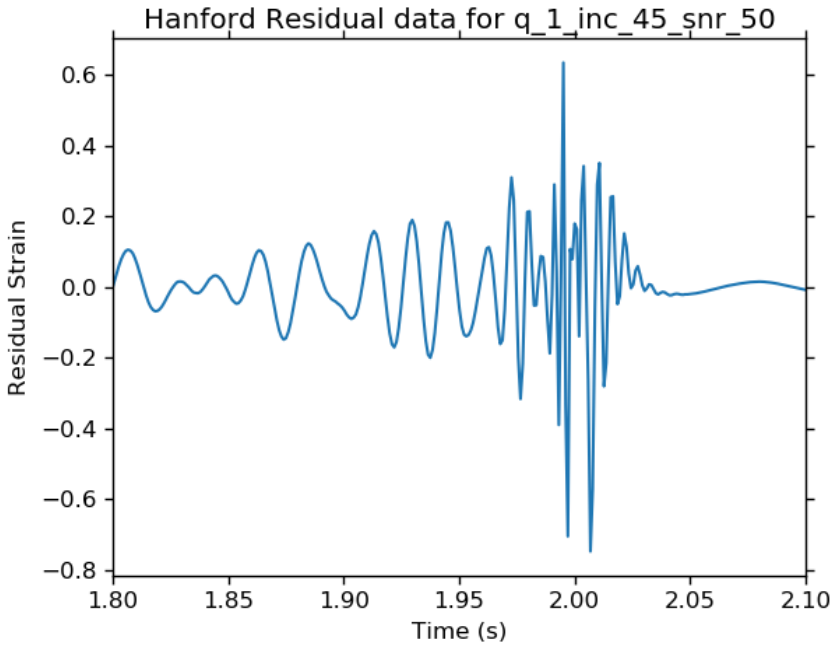

Figure 15. Ringdown plot for the Hanford detector. Waveform has parameters: mass ratio=1, inclination=45°, and SNR=50.

Similar to the ringdown plots for the strain and frequency data, the ringdowm plots for the residual strain data focuses more on the merger-ringdown region of the waveforms. It can be seen more clearly that there is a consistent amount of residual strain around the time of the merger and ringdown phases of the waveform. It would appear that even though the residual strain in the inspiral of the waveform goes down with higher SNR value, the residual strain around the merger-ringdown seems to persist for increasing SNR regardless of inclination.

Test group

The test group for this stage of the study was a set of injection waveforms that had a mass ratio of five. At this mass ratio, the effects of amplitude modulation, and thus increased signal complexity, should become apparent in the data.

Median Overlap

The data presented here is for median overlap that has been collected for both detectors for all SNR values tested, which include 10, 20, 30, 40, and 50, for all inclination angles tested, which include 0, 45, 90, 135, 180, 225, 270, 315, and 360 degrees. For each detector, all the median overlap data with corresponding error bars is presented in a single plot showing the trend of median overlap as a function of SNR for each inclination angle and is shown in Figure 16. for the Hanford detector and in Figure 17. for the Livingston detector. The Livingston data is presented here for completeness of the median overlap data for the test group.

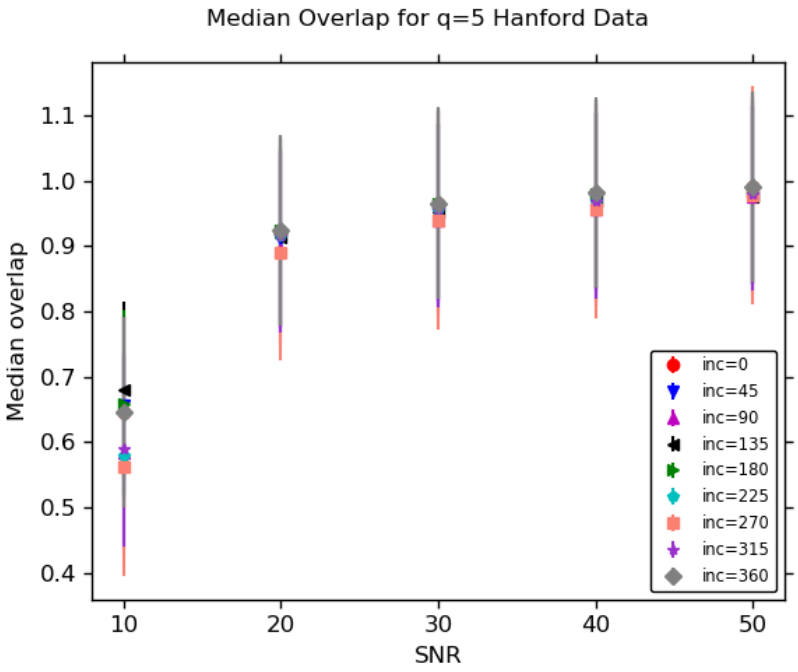

Figure 16. Median Overlap Plot for Hanford Data for Test Group

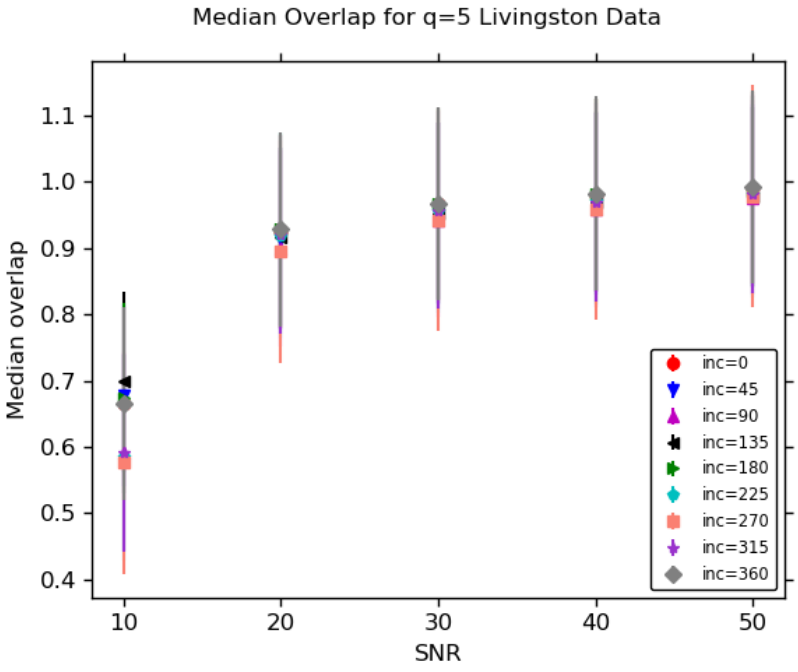

Figure 17. Median Overlap Plot for Livingston Data for Test Group

The median overlap data represents the median network overlap value with respect to the original injection waveform for the one hundred reconstructions that are produced from Bayeswave analysis for the original injection waveform. Thus, it gives a quantitative value for comparing the reconstructions and the injection waveforms. The error bars represent one standard deviation of the set of network overlap for all one hundred of the reconstructions. Even though the data is not as closely spaced for a given SNR like the control group, the median overlap plot suggest that inclination only has a noticeable effect on the median overlap for lower SNR values. The data seems to be somewhat consistent with the control group for high SNR values which suggests that inclination angle has less effect on median overlap and thus the recovery of the injection waveform by the Bayeswave reconstruction for waveforms with higher SNR values where Bayeswave is effective at producing reconstructions [9].

Strain and Frequency Timeseries

The data presented here is for the strain and frequency timeseries collected for all SNR values tested, which include 10, 20, 30, 40, and 50, for all inclination angles, which include 0, 45, 90, 135, 180, 225, 270, 315, and 360 degrees. The data can largely be summarized by presenting plots for a few inclination values since the median overlap plots in the previous section show that inclination seems to have some effects on Bayeswave's effectiveness.

As with the control group, two set of plots were produced and are given the same designation, namely inspiral plots and ringdown plots. The data corresponding to the injection waveform with mass ratio 5, inclination angle of 0, 45, and 90 degrees, and SNR 50 will be considered to express the general trend in the data. The waveforms with

SNR 50 are chosen since they have been shown in the control group to best characterize the waveform and since Bayeswave is expected to be more effective at higher SNR values [9]. Also, it will allow for a better understanding of just how much inclination plays a role in the signal recovery since it was shown higher SNRs did not express much difference in median overlap for the various inclination angles. The data for the inclination angle of 0 degrees is largely similar to the control group in regards to the observed regular amplitude of the waveform before and after the merger as shown in Figure 18.

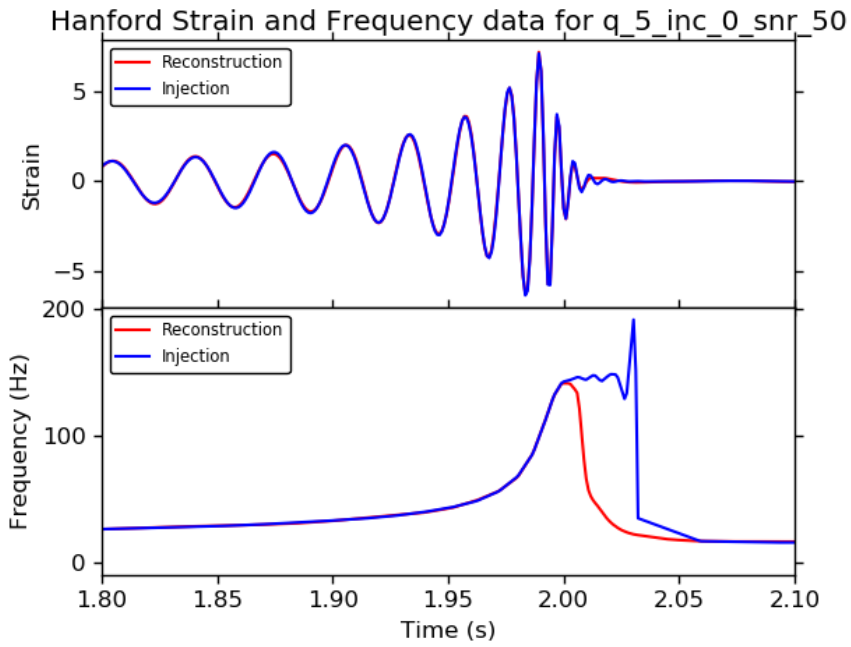

Figure 18. Ringdown plot for the Hanford detector. Waveform has parameters: mass ratio=5, inclination=0°, and SNR=50.

Only the ringdown plot is presented for the waveform with an inclination of 0 degrees because the inspiral does not show any significant sign of deviation between the reconstruction and injection waveforms thus the ringdown is the more significant region for error. As with the control group, there is a noticeable amount of error in the ringdown

region of the waveform displayed in frequency data, so there is an issue with the ringdown recovery.

The waveforms corresponding to inclination angles of 45 and 90 degrees are not so regular in their morphology. Firstly, the inspiral of both waveforms shows discrepancies between the reconstruction and the injection strain, particularly in the inspiral, as show in Figure 19. and Figure 20., respectively.

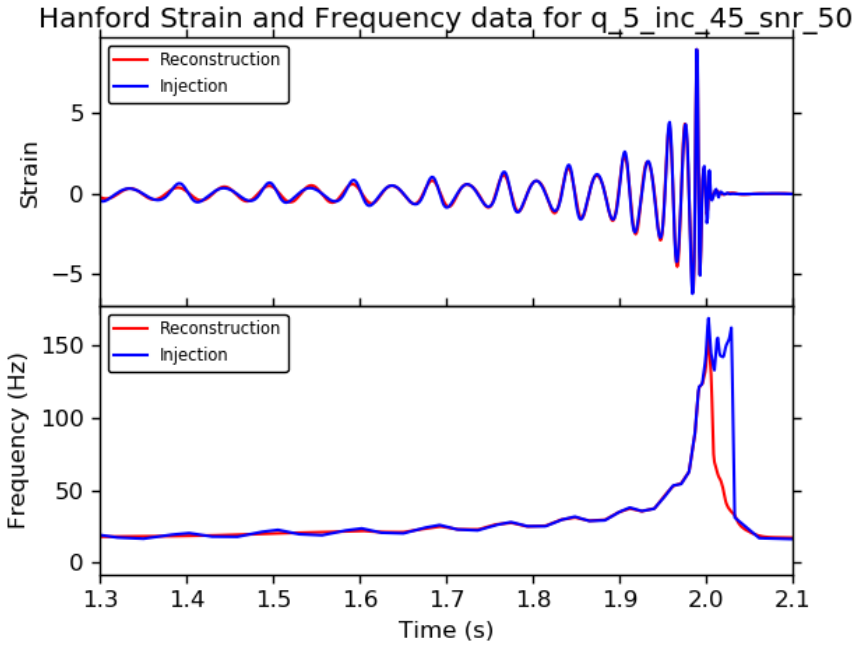

Figure 19. Inspiral plot for the Hanford detector. Waveform has parameters: mass ratio=5, inclination=45°, and SNR=50.

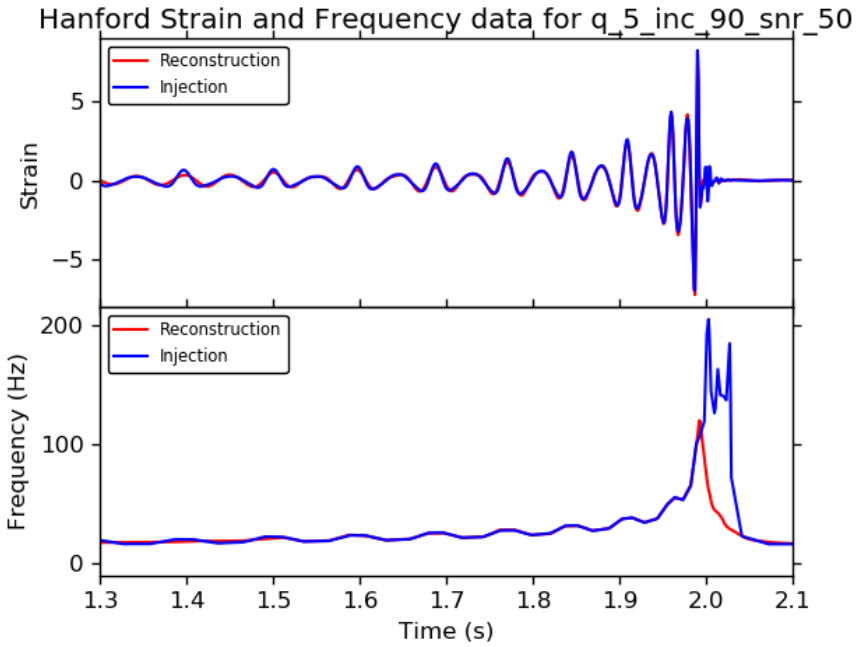

Figure 20. Inspiral plot for the Hanford detector. Waveform has parameters: mass ratio=5, inclination=90°, and SNR=50.

As can be seen in the frequency plot the reconstruction data seems to be rather monotonic in the inspiral region of the waveform for both inclination angles whereas the injection waveform appears to oscillate. Thus, there is some discrepancy with the reconstruction recovering the inspiral data.

Through looking at the ringdown plots it can be seen that there is some noticeable discrepancies between the reconstruction and injection waveforms in the ringdown phase of the waveform as shown in Figure 21. and Figure 22., respectively.

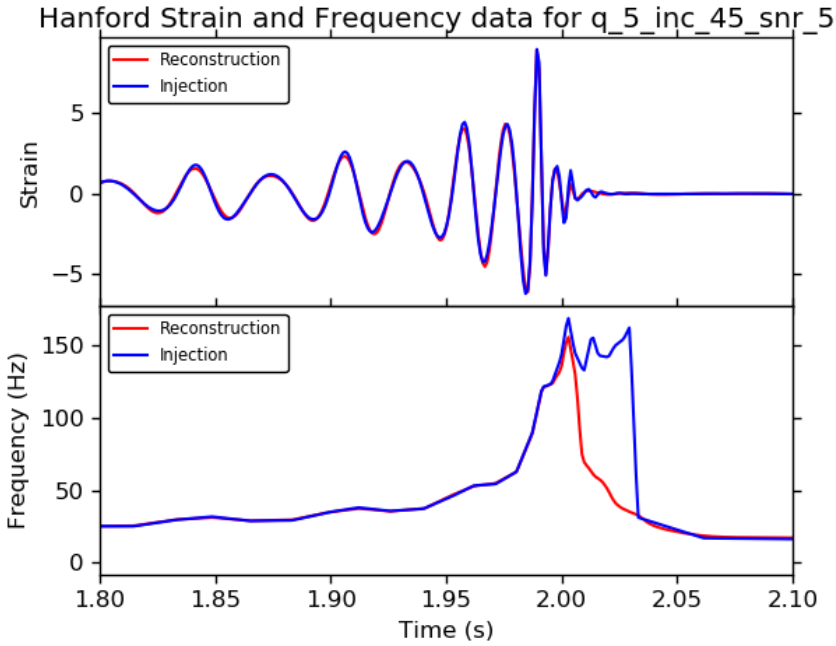

Figure 21. Ringdown plot for the Hanford detector. Waveform has parameters: mass ratio=5, inclination=45°, and SNR=50.

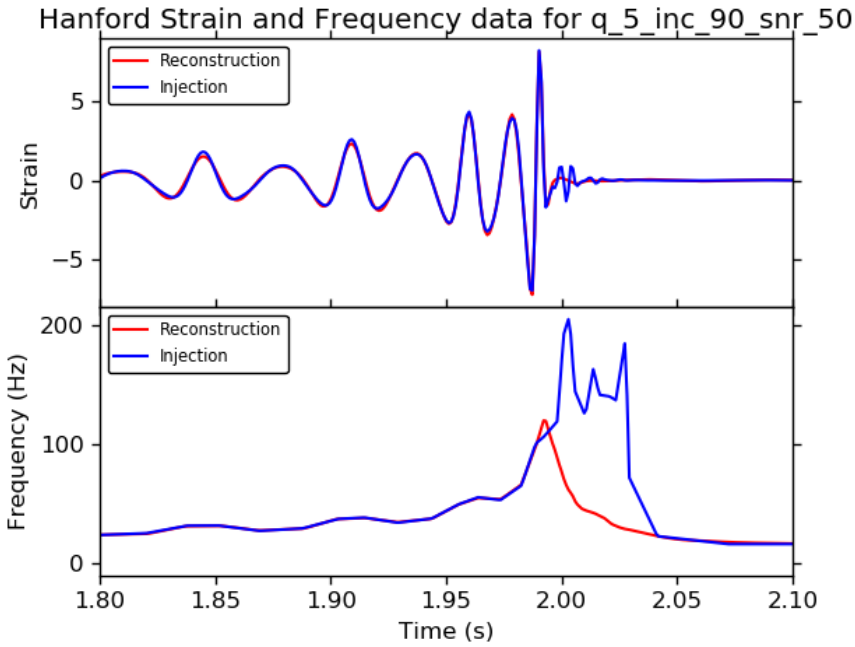

Figure 22. Ringdown plot for the Hanford detector. Waveform has parameters: mass ratio=5, inclination=90°, and SNR=50.

While the reconstruction appears to correspond rather well with the waveform region just before the merger, there are large difference between the reconstruction and injection waveform for the ringdown phase. The discrepancy gets worse when going from inclination angle 0 to 90 degrees which could be a result of higher modes being recovered less as the orientation shifts from face-on to edge-on. This trend is observed for continuing the rotation in inclination angle for each 90-degree rotation increment. The inclination angles of 0, 180, and 360 degrees are similar to the control group waveforms while the largest discrepancies, particularly expressed in the frequency data, can be found for inclination angles of 90 and 270 degrees.

Residual Strain Timeseries

The data presented here is for the residual strain collected for all SNR values tested, which include 10, 20, 30, 40, and 50, for all inclination angles, which include 0,

45, 90, 135, 180, 225, 270, 315, and 360 degrees. The data can largely be summarized by presenting plots for a few inclination values since the median overlap plots in the previous section show that inclination seems to have some effect on Bayeswave's effectiveness.

Taking the waveforms considered in the strain and frequency plots of the test group, looking at the residual plots could give more insight into the degree of the discrepancies in the inspiral and ringdown regions of the waveforms. The ringdown plot for the waveform corresponding to mass ratio 5, inclination angle of 0 degrees, and SNR value of 50 is shown in Figure 23.

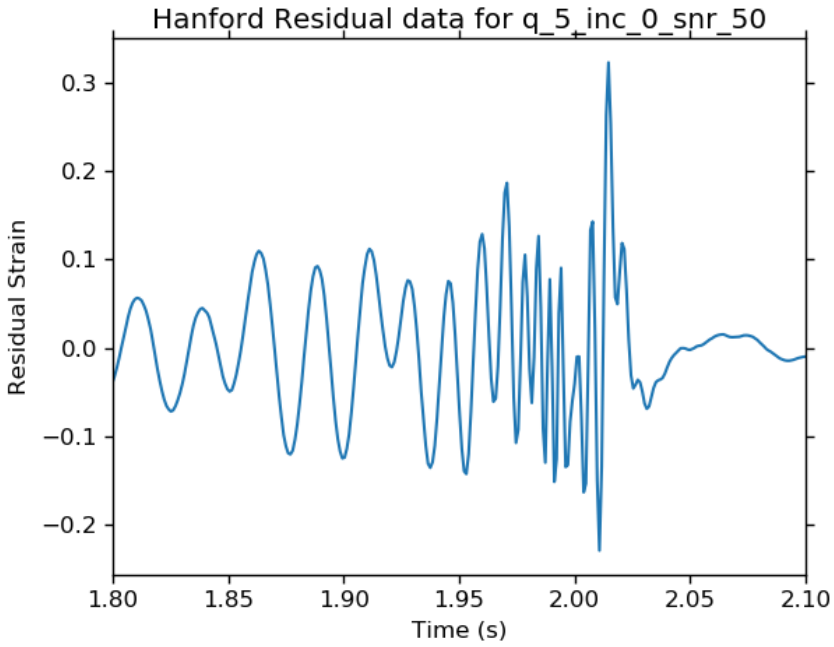

Figure 23. Ringdown plot for the Hanford detector. Waveform has parameters: mass ratio=5, inclination=0°, and SNR=50.

Unlike with its corresponding strain and frequency plot, the ringdown residual plot for the waveform in Figure 23. seems to recover the injection even better than in the similar waveform in the control group when considering the amount of residual remaining.

However, the residual strain data for the waveforms with mass ratio 5, inclination angles 45 and 90, and SNR value of 50, seem to display how severe the discrepancy between the injection and reconstruction are when obvious amplitude modulations are present. The inspiral plot for the two aforementioned waveforms are shown in Figure 24. and Figure 25., respectively.

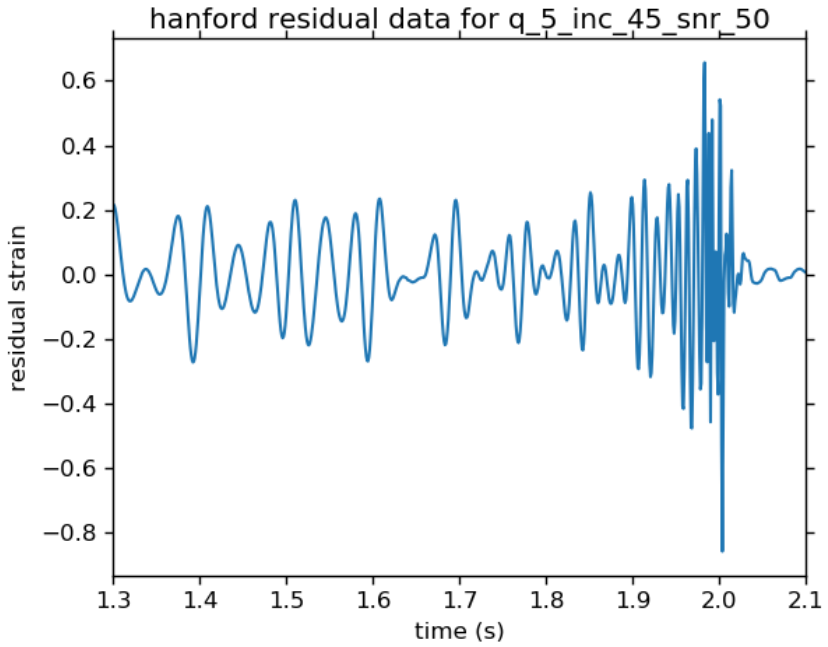

Figure 24. Inspiral plot for the Hanford detector. Waveform has parameters: mass ratio=5, inclination=45°, and SNR=50.

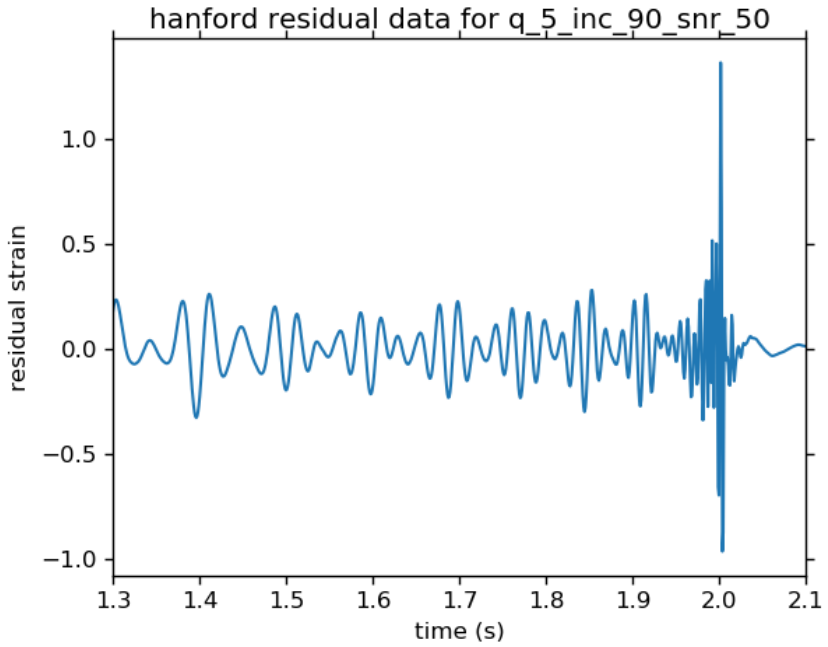

Figure 25. Inspiral plot for the Hanford detector. Waveform has parameters: mass ratio=5, inclination=45°, and SNR=50.

The strain and frequency inspiral plots for these waveforms show that the reconstructions do not seem to recover the amplitude modulations in the injection waveforms. Thus, it can also be observed in the oscillating nature of the residual for the inspiral region of the waveform. However, it appears that most of the residual is located around the ringdown.

For a clearer view of the merger and ringdown region of the waveforms, the ringdown plots for the waveforms with mass ratio 5, inclination angle 45 and 90, and SNR value of 50 are shown in Figure 26. and Figure 27., respectively.

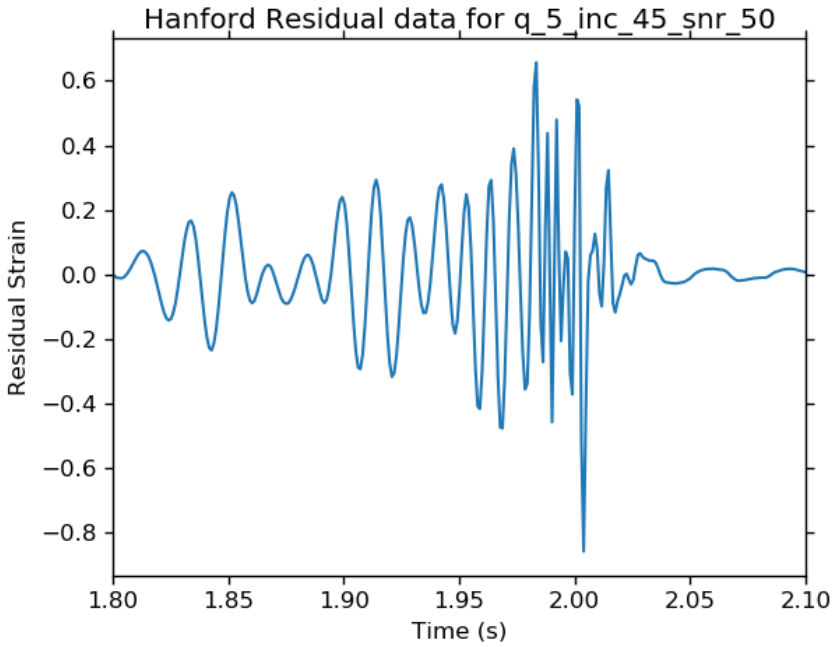

Figure 26. Ringdown plot for the Hanford detector. Waveform has parameters: mass ratio=5, inclination=45°, and SNR=50.

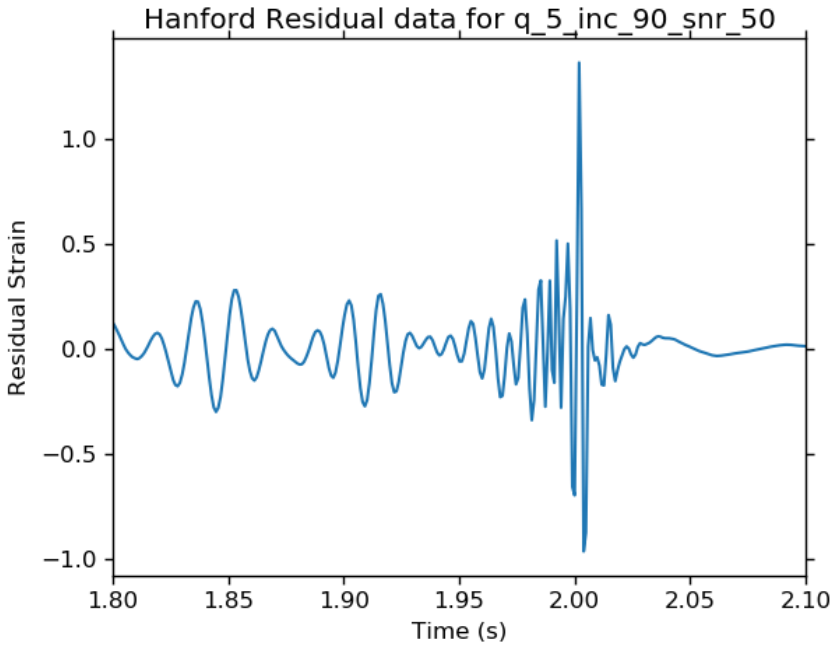

Figure 27. Ringdown plot for the Hanford detector. Waveform has parameters: mass ratio=5, inclination=90°, and SNR=50.

From noticing the magnitude of the residual around the merger and ringdown, it is clear that most of the discrepancy between the injection and reconstruction waveforms is

located here. This is correlated with the strain and frequency ringdown plots in that both the strain and frequency data for the reconstruction is doing a poor job of recovering the ringdown phase of the injection waveform. Although the strain and frequency ringdown plots seem to show a trend as far as how well the injection waveform is recovered as a function of inclination angle for an SNR value of 50, the residual strain plots do not have such a trend. The magnitude of the residual strain peaks for inclination angles of 90 and 135 degrees and actually gets rather low for an inclination angle of 270 degrees, whereas it would be expected that the inclination angles of 90 and 270 degree would be rather similar since they are both in principle edge-on orientations.

The results seem to display different features of the waveforms depending on if one is looking at the strain and frequency plots or the residual strain plots. This is useful since it allows for the data to be analyzed in a more localized way to see where the discrepancies between the injection and the reconstruction mainly reside. From the test group, it is found that the residual strain is greatest for inclination angles of 90 and 135 degrees while it is lowest at inclination angles of 0, 270, and 360 degrees for the Hanford data.

CHAPTER 5

DISCUSSION

With the data collected and analyzed there are some points of discussion that can be made for some of the behavior observed in the gauge plots. The data for the control group was rather consistent with expectations with some exceptions, however there were some interesting trends noticed in the test group gauge plots.

Control Group

The control group does not show any signs of increased signal complexity, such as amplitude modulations in the strain data. These modulations would become more noticeable with more complex initial system parameters, such as in the unequal mass system of the test group. However, there are trends that are observed in the control group that can be discussed in regards to expected trends in the data.

Within the median overlap plots, it seems that for all inclination angles the median overlap between the injection and reconstruction tend toward one, meaning a more accurate overlap since an overlap of one is a perfect match, for increasing values of SNR. This is an expected result in that with a higher SNR value the injected signal is in principle clearer in the data therefore Bayeswave analysis should be able to identify it better and thus produce a more accurate reconstruction. Thus, the median overlap data for the control group suggests that Bayeswave is reconstructing the injection waveforms better for increasing SNR as expected. The error bars for each of the median overlap data points contain all of the other data points relating to the other inclination angles tested. Therefore, this supports the conclusion that the median overlap follows the expected

trend for all inclination angles in the inclination angle does not have much effect on median overlap between the injection and reconstruction waveforms.

Through the strain and frequency plots, it can be observed more directly how well the reconstruction recovers the injection waveform. The two sets of plots, namely the inspiral and ringdown plots, allow for both the inspiral and merger-ringdown regions of the waveforms to be observed separately. As with the median overlap data, the injection and reconstruction strain data appears to overlap more precisely with increasing SNR. This trend can be observed both in the inspiral as well as the ringdown plots, however there are some discrepancies present. With the trend of the overlap becoming very close to one for the injection waveforms, regardless of their inclination angle, corresponding to an SNR value of 50, analyzing the strain and frequency plots for these waveforms would express how well Bayeswave recovers the injected waveform for ideal conditions, such as at higher SNR values.

The inspiral strain and frequency plots for the waveforms corresponding to an SNR value of 50 express that the inspiral seems to be recovered rather well. However, it is clear in both the inspiral and ringdown plots that there is a discrepancy between the reconstruction and injection waveform near the merger-ringdown section of the waveform, especially in the frequency timeseries data. A potential reason for this discrepancy is that the injection waveform has a rather complex waveform structure in the ringdown region. This localized increase in the signal complexity due to the signal being exponentially damped could require a large number of wavelets to reconstruct properly, however Bayeswave might not consider this an optimal number of wavelets for the waveform in its reconstruction and thus is it not recovered properly. This could be

something to focus on in later studies since it is important that Bayeswave be able to accurately recover as much of the waveform as possible. This also seems to somewhat contradict the expectation that Bayeswave accurately recovers simple waveforms, however it could be an indication of something else wrong with the code being used. Considering that Bayeswave is more accurate for high SNR values it could be argued that an SNR value of 50 is not high enough for Bayeswave to even recover simple waveforms accurately [9]. Therefore, this could be a focus for later studies to see what is the threshold SNR for accurate recovery of ringdown.

The residual strain plots follow a similar trend as the strain and frequency plots since the amount of residual strain between the injection and reconstruction waveform becomes less, which means the reconstruction better recovers the injection waveform, with increasing SNR values. However, an observation to potentially note for later trials is that for the inspiral residual plots with low SNR values, regardless of inclination, there seems to be apparent structure within the residual strain data. This could be a result of Bayeswave having a difficult time recovering the beginning section of the injection waveform. Since this seems to not be an issue for the reconstructions with higher SNR values it is most likely just the inability of Bayeswave to extract the inspiral portion of the data for such low SNR values. Therefore, this should be taken into consideration during the analysis of more complex waveform injections and is one of the reason that the waveforms with SNR 50 were focused on in the test group section of the results.

This is corroborated with the inspiral strain and frequency plots in that for increasing SNR values, the reconstruction is able to recover more and more of the inspiral data from the injection waveform. The residual data, for both the inspiral and

ringdown plots, also expresses the largest discrepancy in the data being localized around the merger-ringdown region of the waveform, even for the best recovered waveforms which correspond to an SNR value of 50. This localized increase in residual strain supports the observation noticed in the strain and frequency ringdown plots that the reconstruction is not recovering the localized signal complexity in the merger-ringdown region of the injection waveform. Therefore, the strain and frequency plots are consistent with the residual strain plots which is important for them both to be used together as meaningful gauges of how well the reconstruction recovers the injection waveform.

Even though there is a somewhat large, unexpected discrepancy between the reconstruction and injection waveform for the merger-ringdown section of the waveform, the plots suggest that Bayeswave recovers the injection waveform well given that the median overlap approach near one for the higher SNR values tested regardless of inclination angle. Despite the consistent merger-ringdown discrepancy, the data for the control would suggest that there is little to no effect of Bayeswave's effectiveness at recovering injected signals based on the inclination angle of the injected signal for simple, equal mass systems.

Test Group

The test group appears to show increased signal complexity through amplitude modulations for a majority of the waveforms but not all. The waveforms corresponding to an inclination angles of 0, 180, and 360 degrees express signal morphology to the control group waveforms. This would be expected in that this inclination angles correspond to face-on and anti-face-on orientations which express more simple signal morphologies even for unequal mass systems. Also, in this orientations information regarding the

higher modes of the waveforms would be suppressed thus also limiting the waveform complexity.

The median overlap plots suggest that the reconstruct recovers the injection better with higher SNR values, which as with the control group is what would be expected since more information can be extracted from the signal with increasing SNR. However, the variance of the median overlap for the differing inclination angles is larger for lower SNR value waveforms, which could be expected since the variations in inclination angles will have an effect for the signal complexity for unequal mass systems like those considered in the test group. However, since the overlap was best for injections with an SNR value of 50, that was the focus of the test group results since it would best express how well the reconstruction was recovering the injection waveform.

As was aforementioned, the waveforms corresponding to inclination angles of 0, 180, and 360 degrees all expressed both inspiral and ringdown strain and frequency plots that were similar to those found in the test group since they did not express any amplitude modulations. They recovered the waveform well except for in the merger-ringdown region similar to the control group. However, for the other inclination angles there are some trends that are apparent with the amplitude modulations being present. As shown in Figure 19. and Figure 20., respectively, the inspiral plots for both the waveforms with inclination angle 45 and 90 degrees the reconstruction appears rather monotonic in the inspiral region of the frequency plots of the waveform while the injection frequency data oscillates. This is the first noticeable difference between the reconstruction and injection waveforms for waveforms in the test group displaying amplitude modulations. The deviation in the inspiral could be the results of Bayeswave not being able to properly

capture the earlier inspiral region of the injection waveform despite the SNR of the injection being 50, which was the maximum value tested in this study. This conclusion is supported in that as the SNR of the injection increases for a given mass ratio and inclination angle it can be seen in the strain plots that the reconstruction recovers more and more of the inspiral region of the injection waveform.

Along with the deviation in the inspiral region of the waveform, the ringdown plots for the strain and frequency data express that the large discrepancy in the merger-ringdown region of the waveform since in the control group is also present for the test group waveforms. However, there is more structure in the injection frequency data near the merger-ringdown region of the waveform which is most likely due to the amplitude modulations. The strain data in the ringdown plots suggest that there is congruency between the injection and reconstruction waveform, however the discrepancies are emphasized in the frequency data. Although it was shown that the discrepancy in the merger-ringdown region of the waveform is present in the control group it appears the discrepancy is greater for the test group waveforms. Inclination angle seems to be playing a factor in that the discrepancy grows as the inclination angle is increased from 0 to 90 degrees for the waveforms with an SNR value of 50. This can correlate with the fact that the signal complexity increases due to the potential expression of higher modes in waveforms that deviate from a "face-on" type orientation, namely inclination angles of 0, 180, and 360 degrees, with the highest discrepancies being expressed by the "edge-on" type orientations, namely inclination angles of 90 and 270 degrees. The trend in the discrepancy data supports this claim in that when the system diverges from "face-on" type orientations the amplitude modulations increase, which could be a product of higher

modes in the waveform being expressed, and the increased complexity in the merger-rigndown region of the injection waveform is being poorly recovered by Bayeswave since it potentially would require a large number of wavelets to reconstruct. Or, as was mentioned in for the control group, the SNR threshold to recover the ringdown data has not been reached even by the higher SNR value used in this study, namely an SNR value of 50.

Finally, the residual strain plots help to support the claims made from the strain and frequency for both the insprial and ringdown plots. The residual strain inspiral plots for inclination angles of 45 and 90 degrees express some structure in the inspiral region of the waveform which would correlate with the deviation in the monotonic reconstruction and oscillating injection data for the inspiral region of the waveform observed in the inspiral frequency plots. Also, for the ringdown plots, the residual strain around the merger-ringdown region increases with inclination from 0 to 90 degrees which is consistent with the discrepancy observed in the ringdown plots for the frequency data. However, it is unexpected that the greatest residual strain corresponding to the merger-ringdown region of the waveform for an SNR value of 50 are found for inclination angles of 90 and 135 degrees while the lowest are 0, 270, and 360 degrees. This seems a bit inconsistent with the observations of the ringdown plots for the strain and frequency data for the corresponding waveforms. However, since the strain and frequency data and residual strain data plots are qualitative gauges of complexity recovery it is somewhat difficult to make more concrete conclusion without another quantitative gauge.

Conclusions of Study

The data collected for the control and test groups of this study suggests some detail about Bayeswave reconstructions that could be useful to expand upon in future studies. Firstly, despite the injection waveforms in the control group being recovered rather well from the median overlap plots there was the issue of the discrepancy noticed for the frequency data corresponding to the merger-ringdown region of the waveform. This discrepancy is present in all the control group waveforms regardless of SNR value or inclination angle. Therefore, this would indicate that is not a function of the test parameters but some within the Bayeswave analysis itself that is problematic at recovering that region of the injection waveform. This discrepancy is also present in the frequency data to some extent for all test group waveforms regardless of SNR value or inclination angle. This could also be indicative of an issue with the threshold SNR value at which Bayeswave is effective not being reached to recover the ringdown data since it is exponentially damped or that due to it being exponential damped it might take more wavelets to recover than Bayeswave deems optimal.

Secondly, there is point of interest in the amplitude modulations in the test group waveforms that do not seem to be recovered completely even for the higher SNR value tested for the waveforms that presented amplitude modulations. The amplitude modulations also seemed to introduce more structure into not only the frequency data for the inspiral region of the waveform, but the merger-ringdown as well which complicated the discrepancy already noted for that region of the waveform.

Finally, through analyzing the residual strain inspiral and ringdown plots there seems to be some unexpected results as far as which waveforms have the largest

magnitude of residual strain. However, this will hopefully could be explained or quantified by using a chi squared plot to quantify the residual strain in a similar way as the median overlap for the injection and reconstruction waveforms. The results of the case study seem to be somewhat inconclusive at the current time for a definitive answer on the exact degree to which Bayeswave analysis can recover increased signal complexity in waveform injections. From the data, it would seem that it can recover some, however future studies will need to further quantify if the recovery is good enough.

Future Work

Future work that can be done to further investigate the effectiveness of Bayeswave to recover increased signal complexity could include various things. Perhaps an important step would be understanding why the reconstruction seems to be having such a discrepancy with the injection waveform in the merger-ringdown region of the waveform for even the control group waveforms. Also, it would be useful to introduce another quantitative gauge, such as a chi squared plot for the residual strain data, which would make interpreting the difference between the inclination angle clearer for both the control and test groups. With the two previous suggested adjustments being made, more complexity could be introduced by introduce another degree of freedom into the initial parameters, such as spin.

REFERENCES

[1] A. Taracchini, Y. Pan, A. Buonanno, E. Barausse, M. Boyle, T. Chu, G. Lovelace, H.P. Pfeiffer, and M. A. Scheel, *Prototype effective-one-body model for nonprocessing spinning inspiral-merger-ringdown waveforms.* Phys. Rev. D **86**, 024011 (2012).

[2] B. P. Abbott *et al.* (LIGO Scientific Collaboration and Virgo Collaboration) *Observation of Gravitational Waves from a Binary Black Hole Merger.* Phys. Rev. Lett. **116**, 061102 (2016). License information for reprinting can be found here, https://creativecommons.org/licenses/by/3.0/legalcode

[3] B. P. Abbott *et al.* (LIGO Scientific Collaboration and Virgo Collaboration) *Observing gravitational-wave transient GW150914 with minimal assumptions.* Phys. Rev. D **93**, 122004 (2016); Erratum Phys. Rev. D **94**, 069903

[4] B. P. Abbott *et al.* (LIGO Scientific Collaboration and Virgo Collaboration) *Properties of the Binary Black Hole Merger GW150914.* Phys. Rev. Lett. **116**, 241102 (2016)

[5] B. P. Abbott *et al.* (LIGO Scientific Collaboration and Virgo Collaboration) *Tests of general relativity with GW150914.* Phys. Rev. Lett. **116**, 221101 (2016)

[6] N. Cornish, and T. B. Littenberg, *Bayeswave: Bayesian Interference for Gravitational Wave Bursts and Instrument Glitches.* Classical and Quantum Gravity **32**, 13 (2016)

[7] R. Baltz, *Extraction of Signals in the Presence of Strong Noise: Concepts and Examples.* Frontier Developments in Optics and Spectroscopy (2007)

[8] T. A. Apostolatos, *Search templates for gravitational waves from precessing, inspiraling binaries.* Phys. Rev. D **52**, 2 (1995)

[9] T. B. Littenberg, J. B. Kanner, N. J. Cornish, and M. Millhouse, *Enabling high confidence detections of gravitational-wave bursts.* Phys. Rev. D **94**, 4 (2016)

VITA

Brian Day

DAY was born in Dallas, Georgia. He attended public elementary, middle, and high school in Dallas, Georgia before moving to Atlanta, for university. He will receive a B.S. in physics with a concentration in astrophysics from the Georgia Institute of Technology in May 2017. Mr. Day will be attending the Georgia Institute of Technology to pursue a PhD in physics in Fall 2017. When he is not working on his research, Mr. Day enjoys sketching and hiking.